PID Tracking Control under Multiple Description Encoding Mechanisms

Di Zhao, Zidong Wang, Shuai Liu, Qing-Long Han and Guoliang Wei

***Abstract*—In this paper, a PID tracking control problem is studied for a class of linear discrete-time systems under multiple description encoding mechanisms (MDEMs). The data transmissions on the sensor-to-controller channels are subject to packet dropouts whose occurrences are random and governed by two Bernoulli-distributed sequences of certain probability distributions. In order to improve the reliability of data transmission, an MDEM is put forward, with which the data is encoded into two descriptions of identical importance before being transmitted to the decoders through two individual communication channels. The aim of this paper is to develop a PID tracking controller for guaranteeing the ultimate boundedness of the resulting tracking error, and the corresponding controller gains are obtained by solving an optimization problem. Moreover, the effect of the packet dropouts on the decoding accuracy is explicated via assessing the boundedness in respect to the decoding error. A simulation example is finally presented to showcase the applicability of the proposed PID tracking control scheme.**

***Index Terms*—PID control, tracking control, multiple description encoding mechanism, randomly occurring packet dropout.**

Abbreviations and Notations

PID	Proportional-integral-derivative
MDEM	Multiple description encoding mechanism
ROPD	Randomly occurring packet dropout
EUBMS	Exponentially ultimately bounded in mean-square sense
AUB	Asymptotic upper bound
$\mathbb{R}^p$	The p-dimensional Euclidean space
$\|x\|_2$	The Euclidean norm of x
$\|x\|_\infty$	The infinite norm of x
$\mathbf{0}$	The zero matrix
$\mathbf{I}$	The identity matrix
$\mathscr{X} \geqslant \mathscr{Y}$	$\mathscr{X}$-$\mathscr{Y}$ is positive semi-definite
$\mathscr{X} > \mathscr{Y}$	$\mathscr{X}$-$\mathscr{Y}$ is positive definite
$\lambda_{\max}(\mathscr{M})$	The maximum eigenvalue of a symmetric matrix $\mathscr{M}$
$\lambda_{\min}(\mathscr{M})$	The minimum eigenvalue of a symmetric matrix $\mathscr{M}$
$\mathbb{E}\{\cdot\}$	The expectation operator
$\otimes$	The Kronecker product
$\langle \frac{x}{y} \rangle$	The remainder obtained on dividing x by y
$\lfloor \frac{x}{y} \rfloor$	The quotient obtained on dividing x by y

This work was supported in part by the National Natural Science Foundation of China under Grants 62103281, 61933007, 61903253, and 62273239; the Royal Society of the U.K.; and the Alexander von Humboldt Foundation of Germany. *(Corresponding author: Shuai Liu.)*

Di Zhao is with the College of Science and the Biomedical Engineering Postdoctoral Research Mobile Station, University of Shanghai for Science and Technology, Shanghai 200093, China. (e-mail: zhaodi0907520@163.com)

Zidong Wang is with the Department of Computer Science, Brunel University London, Uxbridge, Middlesex, UB8 3PH, United Kingdom. (e-mail: Zidong.Wang@brunel.ac.uk)

Shuai Liu is with the College of Science, University of Shanghai for Science and Technology, Shanghai 200093, China. (e-mail: liushuai871030@163.com)

Qing-Long Han is with the School of Science, Computing and Engineering Technologies, Swinburne University of Technology, Melbourne, VIC 3122, Australia. (e-mail: qhan@swin.edu.au)

Guoliang Wei is with the Business School, University of Shanghai for Science and Technology, Shanghai 200093, China. (e-mail: guoliang.wei@usst.edu.cn)

I. Introduction

As a fundamental research topic in the control field, the output tracking control problem aims to force the controlled output of the plant, via an appropriate control scheme, to follow the desired reference signal as close as possible. Up till now, output tracking has found a plethora of successful applications in various domains which include, but are not limited to, missile guidance, mobile robots, and aerospace [13], [17], [18]. Accordingly, the tracking control problem has spurred a surge of research effort leading to many excellent results published in the literature [30], [40], [42]. For instance, the tracking control problem has been investigated, respectively, for Takagi-Sugeno fuzzy systems [29], Boolean control networks [47], and high-order nonlinear systems [26].

Since it was first proposed in the 1910s, the PID control strategy has been extensively applied in more than 90% of industrial control loops [1], [2]. To date, the PID controller has been playing a major role in multifarious industrial control processes such as flight control, instrumentation, motor driver and automotive vehicle [11]. Compared with the existing control methods (e.g. the conventional state feedback control algorithm [36], [46]), the PID control method owns the following significant superiorities: 1) the concise mechanism merits the easy-to-implement feature without having to rely on advanced mathematical knowledge; 2) a large number of effective tuning methods are available as a result of the century-long history of the PID control; and 3) the simultaneous utilization of three actions (i.e. the P, I and D actions) makes it possible to pursue superior control performance such as transient behavior, steady-state property as well as robustness, see e.g. [8], [25], [28], [31] and the references therein.

Along with the quick revolution of digital network technologies, the last few decades have seen an increasing popularity of the network-based communication due to their advantages of decreased hard-wiring, convenient installation, and cost-saving in implementation [6], [7], [9], [10], [24], [39]. Nevertheless, the inherently limited bandwidth of communication networks

This article has been accepted for publication in a future issue of this journal, but has not been fully edited. Content may change prior to final publication. Citation information: DOI10.1109/TSMC.2023.3290011 IEEE Transactions on Systems, Man, and Cybernetics: Systems

may cause data collision, network congestion and even packet dropouts [19], [27], [32]. Such kinds of phenomena, if not addressed, would seriously jeopardize the system performance [37], [41], [43]–[45], [48]. In this regard, appropriate data transmission mechanisms have been exploited with aim to modulate the signal transmission, thereby better utilizing the limited network resource and mitigating the adverse effects resulting from the network-induced phenomena [16], [21], [22], [35].

Among various transmission mechanisms, the MDEM has been widely applied in distributed storage systems, diverse communication systems and image/audio/video encoding [3], [5], [12], [14], [15], [23], [34]. Under MDEMs, the data is encoded into multiple descriptions with identical importance, and then the multiple description packets are transmitted to the decoder through parallel independent channels. Clearly, the more descriptions available to the decoder (i.e., the more normally operating channels), the smaller decoding errors and, subsequently, the higher decoding accuracy. Accordingly, the utilization of the MDEMs would help enhance the reliability of data transmission, and this is especially true when the communication channels suffer from packet dropouts. Nevertheless, despite its practical importance, the MDEM-based control problem has not gained much research attention yet, let alone the case when output tracking control and PID control are also addressed. Such a lack of adequate results is mainly due to the mathematical challenges caused by the co-existence of the packet dropout, the decoding errors as well as the reference input.

Motivated by the discussions made thus far, we are motivated to tackle the PID tracking control problem for a class of linear discrete-time systems under MDEMs. In doing so, three foreseeable challenges emerge as follows: 1) how to develop an effective PID tracking controller to ensure the ultimate boundedness of tracking error? 2) how to elevate the reliability of codeword transmission in the presence of ROPDs? and 3) how to explicitly describe the decoding-error-induced effects on the tracking performance? As such, the primary purpose of the current study is to make an endeavor to provide satisfactory answers to these three questions.

The primary contributions we are delivering can be outlined in threefold. *1) To our knowledge, we make one of the first few attempts here to design a PID tracking controller under ROPD and MDEM. 2) In comparison to the existing encoding schemes, the MDEM implemented on the codeword transmission process is more prominent in eliminating/attenuating adverse influences from ROPD onto decoding accuracy. 3) A theoretical framework is established to examine the joint effects of the ROPD, the decoding errors and the disturbance input on the tracking performance in a quantitative way.*

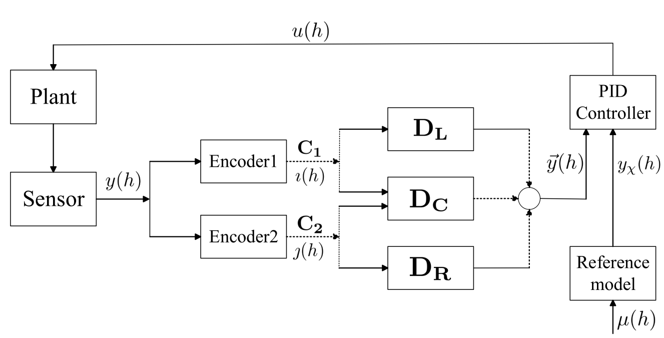

Fig. 1: PID tracking control problem under multiple description encoding mechanism.

The rest of this paper is structured as follows. In Section II, the considered tracking control problem under the MDEM is formulated. In Section III, the PID tracking controller is developed, and the boundedness of decoding error and tracking error are respectively analyzed. Section IV, a numerical example is given to illustrate the usefulness of the proposed PID tracking control scheme, and a few concluding remarks are lastly made in Section V.

II. Problem Formulation and Preliminaries

A. System Model

Consider a class of discrete linear time-invariant systems characterized by the following state-space model:

$$\begin{cases} x(h+1) = Ax(h) + Bu(h) + Mv(h) \\ y(h) = Cx(h) \\ z(h) = Ex(h) \end{cases} \tag{1}$$

where $x(h) \in \mathbb{R}^{p_x}$, $u(h) \in \mathbb{R}^{p_u}$, $y(h) \in \mathbb{R}^{p_y}$ and $z(h) \in \mathbb{R}^{p_z}$ represent, respectively, the system state, the control input, the measurement output and the controlled output; $v(h) \in \mathbb{V} \triangleq \{v : \|v\| \leqslant \bar{v};\ v \in \mathbb{R}^{p_v}\}$ denotes the exogenous disturbance with $\bar{v} > 0$ being a known scalar; and A, B, C, M and E are known matrices with compatible dimensions.

B. Multiple Description Encoding Procedure

In practical engineering, data transmissions often face the phenomenon of packet dropouts due to limited communication capacity. To improve the efficiency of resource utilization, the MDEM is used to alleviate the adverse effects induced by the packet dropouts.

Encoder:

$$\begin{cases} \imath_s(h) = \aleph_{r,s}\big(y_s(h)\big) \\ \jmath_s(h) = \aleph_{c,s}\big(y_s(h)\big) \end{cases} \tag{2}$$

Decoder:

$$\vec{y}_s(h) = \begin{cases} \Re^l_s\big(\imath_s(h)\big), & \text{when } \phi_1(h) = 1,\ \phi_2(h) = 0 \\ \Re^r_s\big(\jmath_s(h)\big), & \text{when } \phi_1(h) = 0,\ \phi_2(h) = 1 \\ \Re^c_s\big(\imath_s(h),\ \jmath_s(h)\big), & \text{when } \phi_1(h) = 1,\ \phi_2(h) = 1 \\ \vec{y}_s(h-1), & \text{when } \phi_1(h) = 0,\ \phi_2(h) = 0 \end{cases} \tag{3}$$

where $\aleph_{r,s}(\cdot)$ and $\aleph_{c,s}(\cdot)$ are two encoding functions; $\Re^l_s(\cdot)$ and $\Re^r_s(\cdot)$ are two side decoding functions and $\Re^c_s(\cdot\,,\,\cdot)$ is the central decoding function; $\imath_s(h)$ and $\jmath_s(h)$ are two individual descriptions of $y_s(h)$ with $y_s(h)$ being the sth component of $y(h)$; $\vec{y}_s(h)$ is the decoding value corresponding to $y_s(h)$ and $s \in \mathfrak{S}\{1, 2, \ldots, p_y\}$. $\phi_\iota(h)$ $(\iota = 1, 2)$ are two independent Bernoulli sequences, which regulate the probabilistic nature of

This article has been accepted for publication in a future issue of this journal, but has not been fully edited. Content may change prior to final publication. Citation information: DOI10.1109/TSMC.2023.3290011 IEEE Transactions on Systems, Man, and Cybernetics: Systems

the packet dropout phenomena in the course of the description transmissions, obey the following probability distributions:

$$\begin{aligned}&\text{Prob}\{\phi_1(h)=1\}=\bar{\phi}_1, \quad \text{Prob}\{\phi_1(h)=0\}=1-\bar{\phi}_1\\ &\text{Prob}\{\phi_2(h)=1\}=\bar{\phi}_2, \quad \text{Prob}\{\phi_2(h)=0\}=1-\bar{\phi}_2.\end{aligned}$$

Here, $\phi_\iota(h)=1$ means that the ιth channel works normally, and $\phi_\iota(h)=0$ corresponds to the scenario of the ιth channel undergoing the packet dropouts at time instant h.

Before presenting the encoder-decoder structure, let us introduce three random variables $\xi_m(h)$ ($m\in\mathfrak{M}\triangleq\{0,\,1,\,2\}$) as follows:

$$\xi_m(h)\triangleq\delta\big(\phi(h),\,m\big), \quad \phi(h)\triangleq\phi_1(h)+\phi_2(h), \tag{4}$$

which satisfy $\sum_{m=0}^{2}\xi_m(h)=1$ and

$$\mathbb{E}\{\xi_0(h)\}=\bar{\xi}_0, \quad \mathbb{E}\{\xi_1(h)\}=\bar{\xi}_1, \quad \mathbb{E}\{\xi_2(h)\}=\bar{\xi}_2 \tag{5}$$

with

$$\begin{aligned}\bar{\xi}_0 &\triangleq(1-\bar{\phi}_1)(1-\bar{\phi}_2)\\ \bar{\xi}_1 &\triangleq\bar{\phi}_1(1-\bar{\phi}_2)+\bar{\phi}_2(1-\bar{\phi}_1)\\ \bar{\xi}_2 &\triangleq\bar{\phi}_1\bar{\phi}_2.\end{aligned}$$

Remark 1: According to (4) and Fig. 1, $\phi(h)=2$ implies that both channels "$\mathbf{C_1}$" and "$\mathbf{C_2}$" work normally and the central decoder "$\mathbf{D_C}$" is triggered to generate the decoded value. $\phi(h)=1$ implies that only one channel ("$\mathbf{C_1}$" or "$\mathbf{C_2}$") works normally and the side decoder "$\mathbf{D_L}$" or "$\mathbf{D_R}$" is activated to execute the decoding procedure. $\phi(h)=0$ implies that the packet dropouts occur in both channels "$\mathbf{C_1}$" and "$\mathbf{C_2}$" and, correspondingly, all the decoders fail to work.

For presentation clarity, we set

$$\begin{aligned}\vec{y}(h)&\triangleq\big[\vec{y}_1(h)\quad\vec{y}_2(h)\quad\cdots\quad\vec{y}_{p_y}(h)\big]^T\\ \imath(h)&\triangleq\big[\imath_1(h)\quad\imath_2(h)\quad\cdots\quad\imath_{p_y}(h)\big]^T\\ \jmath(h)&\triangleq\big[\jmath_1(h)\quad\jmath_2(h)\quad\cdots\quad\jmath_{p_y}(h)\big]^T\\ \Re^l\big(\imath(h)\big)&\triangleq\Big[\Re^l_1\big(\imath_1(h)\big)\quad\Re^l_2\big(\imath_2(h)\big)\ \cdots\ \Re^l_{p_y}\big(\imath_{p_y}(h)\big)\Big]^T\\ \Re^r\big(\jmath(h)\big)&\triangleq\Big[\Re^r_1\big(\jmath_1(h)\big)\quad\Re^r_2\big(\jmath_2(h)\big)\ \cdots\ \Re^r_{p_y}\big(\jmath_{p_y}(h)\big)\Big]^T\\ \Re^c\big(\imath(h),\jmath(h)\big)&\triangleq\big[\ \Re^c_1\big(\imath_1(h),\jmath_1(h)\big)\quad\Re^c_2\big(\imath_2(h),\jmath_2(h)\big)\\ &\qquad\cdots\quad\Re^c_{p_y}\big(\imath_{p_y}(h),\jmath_{p_y}(h)\big)\ \big]^T.\end{aligned}$$

The scalar-valued encoder-decoder pair (2)-(3) can be compacted into the following form:

$$\begin{cases}\imath(h)=\aleph_r\big(y(h)\big)\\ \jmath(h)=\aleph_c\big(y(h)\big)\end{cases} \tag{6}$$

and

$$\vec{y}(h)=\begin{cases}\Re^c\big(\imath(h),\,\jmath(h)\big), & \text{when } \phi_1(h)=1,\ \phi_2(h)=1\\ \Re^r\big(\jmath(h)\big), & \text{when } \phi_1(h)=0,\ \phi_2(h)=1\\ \Re^l\big(\imath(h)\big), & \text{when } \phi_1(h)=1,\ \phi_2(h)=0\\ \vec{y}(h-1), & \text{when } \phi_1(h)=0,\ \phi_2(h)=0.\end{cases} \tag{7}$$

Denote the decoding error between the measurement $y(h)$ and the decoded value $\vec{y}(h)$ as $\kappa_m(h)$ with $m\in\mathfrak{M}$ representing the number of received description packets. Accordingly, the decoded measurement output $\vec{y}(h)$ is modeled as:

$$\begin{aligned}\vec{y}(h)=&\xi_0(h)\big(y(h)+\kappa_0(h)\big)+\xi_1(h)\big(y(h)+\kappa_1(h)\big)\\ &+\xi_2(h)\big(y(h)+\kappa_2(h)\big)\\ =&y(h)+\xi_0(h)\kappa_0(h)+\xi_1(h)\kappa_1(h)+\xi_2(h)\kappa_2(h).\end{aligned} \tag{8}$$

C. PID Tracking controller

The aim of this paper is to develop a tracking controller such that the controlled output of the system (1) tracks the controlled output signal of the following system:

$$\begin{cases}\chi(h+1)=F\chi(h)+G\mu(h)\\ y_\chi(h)=H\chi(h)\\ z_\chi(h)=E\chi(h)\end{cases} \tag{9}$$

where $\chi(h)\in\mathbb{R}^{p_\chi}$ and $\mu(h)\in\mathbb{R}^{p_\mu}$ are, respectively, the reference state and the reference input satisfying $\|\mu(h)\|\leqslant\bar{\mu}$ with $\bar{\mu}$ being a known positive scalar; $y_\chi(h)\in\mathbb{R}^{p_y}$ and $z_\chi(h)\in\mathbb{R}^{p_z}$ are the measurement and controlled output of the reference system; and F, G and H are constant matrices with F being Hurwitz.

By setting $\hbar(h)\triangleq\big[\vec{y}^T(h)\quad y_\chi^T(h)\big]^T$, the following PID tracking controller is constructed:

$$u(h)=\mathscr{P}\hbar(h)+\mathscr{I}\sum_{p=h-q}^{h-1}\hbar(p)+\mathscr{D}\big(\hbar(h)-\hbar(h-1)\big) \tag{10}$$

with

$$\mathscr{P}\triangleq\big[P_x\quad P_\chi\big], \quad \mathscr{I}\triangleq\big[I_x\quad I_\chi\big], \quad \mathscr{D}\triangleq\big[D_x\quad D_\chi\big]$$

and P_x, P_χ, I_x, I_χ, D_x, D_χ being the controller gains to be determined.

Remark 2: It is worth noting that the traditional PID controller utilizes all historical information in its integral term, and this might lead to issues with algorithm convergence. To handle such issues, a time window of adjustable length is adopted in the integral term of the developed PID tracking controller, based on which the underlying accumulation error can be approximately tackled with reduced computational burden.

Defining the state tracking error $\varepsilon(h)\triangleq x(h)-\chi(h)$ and the controlled output tracking error $z_\varepsilon(h)\triangleq z(h)-z_\chi(h)$, we have the tracking error system of the following form:

$$\begin{cases}\varepsilon(h+1)=A\varepsilon(h)+(A-F)\chi(h)+Bu(h)\\ \qquad\qquad+Mv(h)-G\mu(h)\\ z_\varepsilon(h)=E\varepsilon(h)\end{cases}. \tag{11}$$

By setting $\flat(h)\triangleq\big[\varepsilon^T(h)\quad\chi^T(h)\big]^T$, we obtain the follow-

This article has been accepted for publication in a future issue of this journal, but has not been fully edited. Content may change prior to final publication. Citation information: DOI10.1109/TSMC.2023.3290011 IEEE Transactions on Systems, Man, and Cybernetics: Systems

ing augmented system:

$$\begin{cases} \flat(h+1) = \mathcal{A}\flat(h) + \mathcal{S}\varrho(h) + \mathcal{W}o(h) \\ \qquad + \mathcal{T}\big(\hat{\Xi}_0 + \tilde{\Xi}_0(h)\big)\iota_0(h) \\ \qquad + \mathcal{T}\big(\hat{\Xi}_1 + \tilde{\Xi}_1(h)\big)\iota_1(h) \\ \qquad + \mathcal{T}\big(\hat{\Xi}_2 + \tilde{\Xi}_2(h)\big)\iota_2(h) \\ z_\varepsilon(h) = \mathcal{E}\flat(h) \\ \flat(j) = 0, \quad j = 0, 1, \ldots, q \end{cases} \tag{12}$$

where

$$\begin{aligned}
\mathcal{A} \triangleq & \mathscr{A} + \mathscr{B}, \quad \mathcal{S} \triangleq \begin{bmatrix} B\mathscr{R}_1\mathscr{C} \\ \mathbf{0} \end{bmatrix}, \quad \mathcal{T} \triangleq \begin{bmatrix} B\mathscr{R}_2 \\ \mathbf{0} \end{bmatrix} \\
\mathcal{W} \triangleq & \begin{bmatrix} M & -G \\ \mathbf{0} & G \end{bmatrix}, \ \mathcal{E} \triangleq \begin{bmatrix} E & \mathbf{0} \end{bmatrix}, \ \mathscr{A} \triangleq \begin{bmatrix} A & A-F \\ \mathbf{0} & F \end{bmatrix} \\
\mathscr{B} \triangleq & \begin{bmatrix} B(P_x + D_x)C & B(P_\chi + D_\chi)(C+H) \\ \mathbf{0} & \mathbf{0} \end{bmatrix} \\
\mathscr{R}_1 \triangleq & \big[\mathscr{I} + \mathscr{D} \quad \underbrace{\mathscr{I} \quad \cdots \quad \mathscr{I}}_{q-1}\big], \quad \mathscr{C} \triangleq \mathbf{I}_q \otimes \mathscr{C}_0 \\
\mathscr{R}_2 \triangleq & \big[P_x + D_x \quad I_x + D_x \quad \underbrace{I_x \quad \cdots \quad I_x}_{q-1}\big] \\
\mathscr{C}_0 \triangleq & \begin{bmatrix} C & \mathbf{0} \\ \mathbf{0} & C+H \end{bmatrix}, \quad o(h) \triangleq \begin{bmatrix} v^T(h) & \mu^T(h) \end{bmatrix}^T \\
\varrho(h) \triangleq & \begin{bmatrix} \flat^T(h-1) & \flat^T(h-2) & \cdots & \flat^T(h-q) \end{bmatrix}^T \\
\iota_0(h) \triangleq & \begin{bmatrix} \kappa_0^T(h) & \kappa_0^T(h-1) & \cdots & \kappa_0^T(h-q) \end{bmatrix}^T \\
\iota_1(h) \triangleq & \begin{bmatrix} \kappa_1^T(h) & \kappa_1^T(h-1) & \cdots & \kappa_1^T(h-q) \end{bmatrix}^T \\
\iota_2(h) \triangleq & \begin{bmatrix} \kappa_2^T(h) & \kappa_2^T(h-1) & \cdots & \kappa_2^T(h-q) \end{bmatrix}^T \\
\hat{\Xi}_0 \triangleq & \mathbf{I}_{q+1} \otimes \bar{\xi}_0, \quad \hat{\Xi}_1 \triangleq \mathbf{I}_{q+1} \otimes \bar{\xi}_1, \quad \hat{\Xi}_2 \triangleq \mathbf{I}_{q+1} \otimes \bar{\xi}_2 \\
\tilde{\xi}_0(h) \triangleq & \xi_0(h) - \bar{\xi}_0, \ \tilde{\Xi}_0(h) \triangleq \text{diag}\{\tilde{\xi}_0(h), \ \ldots, \ \tilde{\xi}_0(h-q)\} \\
\tilde{\xi}_1(h) \triangleq & \xi_1(h) - \bar{\xi}_1, \ \tilde{\Xi}_1(h) \triangleq \text{diag}\{\tilde{\xi}_1(h), \ \ldots, \ \tilde{\xi}_1(h-q)\} \\
\tilde{\xi}_2(h) \triangleq & \xi_2(h) - \bar{\xi}_2, \ \tilde{\Xi}_2(h) \triangleq \text{diag}\{\tilde{\xi}_2(h), \ \ldots, \ \tilde{\xi}_2(h-q)\}.
\end{aligned}$$

Now, we are ready to highlight the purpose of this paper. For linear time-invariant system (1), we are interested in determining the parameters of the PID tracking controller (i.e., P_x, P_χ, I_x, I_χ, D_x, D_χ) such that the output tracking error dynamics $z_\varepsilon(h)$ is EUBMS subject to the process noise $v(h)$, the reference input $\mu(h)$ and the decoding error $\kappa_m(h)$ ($m \in \mathfrak{M}$). More specifically, we would like to design a desired PID tracking controller such that there exist three constants $\theta_i > 0$ ($i = 1, 2, 3$) satisfying

$$\mathbb{E}\{\|z_\varepsilon(h)\|^2\} \leqslant \theta_1^h \theta_2 + \theta_3 \tag{13}$$

where $0 \leqslant \theta_1 < 1$ denotes the decay rate and θ_3 denotes the AUB of $\|z_\varepsilon(h)\|^2$.

III. Main Results

In this section, we first analyze the boundedness of the decoding/tracking error and then provide an executable design algorithm to parameterize the controller gains.

A. Design of Encoding Scheme

In this subsection, the data encoding procedure will be formalized in two steps. The first step (the index generation step) aims to convert the measurement output into the corresponding index by employing the uniform quantization method, and the second step (the index assignment step) endeavors to assign the generated indices to a certain mapping matrix based on the nested index assignment principle.

Step 1. Index Generation

For a scalar uniform quantizer $\acute{o}_s(\cdot) : \mathbb{R} \to \mathbb{R}$ ($s \in \mathfrak{S}$) of the following form:

$$\acute{o}_s(d_s) = \begin{cases} r_s, & d_s \geqslant r_s \\ -r_s, & d_s \leqslant -r_s \\ -r_s + \dfrac{(2g_s - 1)r_s}{l_s}, & -r_s + t_s^- \leqslant d_s \leqslant -r_s + t_s^+ \end{cases} \tag{14}$$

the scaling parameters d_s, r_s and the positive integer l_s correspond to, respectively, the signal to be processed, the saturation value and the quantization level, where

$$\begin{aligned} t_s^- \triangleq & 2(g_s - 1)r_s l_s^{-1}, \quad t_s^+ \triangleq 2g_s r_s l_s^{-1} \\ g_s \in & \mathfrak{L}_{\mathfrak{s}} \triangleq \{1, 2, \ldots, l_s\}. \end{aligned}$$

In the light of (14), the interval $[-r_s, r_s]$ is uniformly partitioned into l_s subintervals, and the ith subinterval of $[-r_s, r_s]$ is defined as

$$\left[-r_s + 2(i-1)r_s l_s^{-1}, \, -r_s + 2ir_s l_s^{-1}\right], \quad i \in \mathfrak{L}_s.$$

In order to avoid the quantizer $\acute{o}_s(\cdot)$ being saturated, an adaptive parameter ϖ_s is introduced into the signal pretreating process. Accordingly, the quantizer output is generated by

$$\acute{o}_s\big(y_s(h)\big) = \varpi_s \acute{o}\big(\frac{y_s(h)}{\varpi_s}\big). \tag{15}$$

In this sense, once $|y_s(h)| > r_s$, $y_s(h)/\varpi_s$ belongs to the interval $[-r_s, r_s]$. Consequently, one can generate the index by the following function:

$$\varsigma_s\Big(\acute{o}_s\big(y_s(h)\big)\Big) = \wp_s(h), \quad \wp_s(h) \in \mathfrak{L}_{\mathfrak{s}}. \tag{16}$$

Denote the quantization error $\pi_s(h) \triangleq y_s(h) - \acute{o}_s\big(y_s(h)\big)$. It follows from (14)-(15) that the quantization error $\pi_s(h)$ satisfies

$$|\pi_s(h)| \leqslant \frac{\varpi_s r_s}{l_s}. \tag{17}$$

Step 2. Index Assignment

For the generated index $\wp_s(h)$, the index assignment function $\vartheta_s(\cdot)$: $\mathbb{N}^+ \to \mathbb{N}^+ \times \mathbb{N}^+$ is constructed as follows to assign $\wp_s(h)$ into an α-dimensional mapping matrix $\mathbf{W}_s$ (α being an even number) :

$$\begin{aligned} & \vartheta_s\big(\wp_s(h)\big) \triangleq \Big(\vartheta_s^r\big(\wp_s(h)\big), \, \vartheta_s^c\big(\wp_s(h)\big)\Big) \\ & = \begin{cases} \big(\tau_s(h)+1, \, \tau_s(h)+1\big), & \text{if } \upsilon_s(h) = 1 \\ \big(\tau_s(h)+1, \, \tau_s(h)\big), & \text{if } \upsilon_s(h) = 0 \text{ and } \tau_s(h) \text{ is even} \\ \big(\tau_s(h), \, \tau_s(h)+1\big), & \text{if } \upsilon_s(h) = 0 \text{ and } \tau_s(h) \text{ is odd} \\ \big(\tau_s(h)+2, \, \tau_s(h)+1\big), & \text{if } \upsilon_s(h) = 2 \text{ and } \tau_s(h) \text{ is even} \\ \big(\tau_s(h)+1, \, \tau_s(h)+2\big), & \text{if } \upsilon_s(h) = 2 \text{ and } \tau_s(h) \text{ is odd} \end{cases} \end{aligned} \tag{18}$$

This article has been accepted for publication in a future issue of this journal, but has not been fully edited. Content may change prior to final publication. Citation information: DOI10.1109/TSMC.2023.3290011 IEEE Transactions on Systems, Man, and Cybernetics: Systems

where

$$\tau_s(h) \triangleq = \lfloor \frac{\wp_s(h)}{2\beta+1} \rfloor = \lfloor \frac{\wp_s(h)}{3} \rfloor,$$
$$\upsilon_s(h) \triangleq = \langle \frac{\wp_s(h)}{2\beta+1} \rangle = \langle \frac{\wp_s(h)}{3} \rangle.$$

Here, $\vartheta_s^r(\cdot)$ and $\vartheta_s^c(\cdot)$ stand for, respectively, the row assignment function and the column assignment function, and $\imath_s(h)$ and $\jmath_s(h)$ denote, respectively, the row location and the location of the cell containing $\wp_s(h)$ in the mapping matrix $\mathbf{W}_s$. Evidently, by means of the index assignment function $\vartheta_s(\cdot)$, the single description $\wp_s(h)$ is converted into the description pair $\big(\imath_s(h),\, \jmath_s(h)\big)$ with

$$\imath_s(h) = \vartheta_s^r\big(\wp_s(h)\big), \quad \jmath_s(h) = \vartheta_s^c\big(\wp_s(h)\big).$$

Based on the above discussion, the encoding functions $\aleph_{r,s}(\cdot)$ and $\aleph_{c,s}(\cdot)$ can be given as follows:

$$\begin{cases} \aleph_{r,s}\big(y_s(h)\big) = \vartheta_s^r\Big(\varsigma_s\Big(\acute{o}_s\big(y_s(h)\big)\Big)\Big) \\ \aleph_{c,s}\big(y_s(h)\big) = \vartheta_s^c\Big(\varsigma_s\Big(\acute{o}_s\big(y_s(h)\big)\Big)\Big). \end{cases} \tag{19}$$

1	3						
2	4	5					
	6	7	9				
		8	10	11			
			12	13	15		
				14	16	17	
					18	19	21
						20	22

Fig. 2: Nested index assignment for $\alpha = 8$ and $\beta = 1$ in [33].

Remark 3: As shown in Fig. 2 and stated in [33], the indices $\wp_s(h)$ $(s \in \mathfrak{S})$ are assigned to the cells lying on the main diagonal and the nearest 2β diagonal of the mapping matrix $\mathbf{W}_s$ according to the nested assignment principle. In this paper, for illustration convenience, we only discuss the scenario of $\beta = 1$, where the indices $\wp_s(h)$ $(s \in \mathfrak{S})$ are assigned to the cells located on the main diagonal and its nearest 2 diagonals of the mapping matrix $\mathbf{W}_s$.

B. Design of Decoding Scheme

In this subsection, we endeavor to establish the decoding scheme through two steps. To begin with, an index estimation strategy is put forward to estimate the index $\wp_s(h)$ $(s \in \mathfrak{S})$ based on the received descriptions. Then, the decoding function is developed according to the estimated index $\hat{\wp}_s(h)$ for the sake of obtaining the decoded value as accurately as possible.

Step 1. Index Estimation

Note that the index $\wp_s(h)$, which is exclusively determined by two descriptions $\imath_s(h)$ and $\jmath_s(h)$, carries essential information of $y_s(h)$, thereby placing a crucial impact on the design of decoding scheme. However, due to the probabilistic packet dropout when transmitting the descriptions $\imath_s(h)$ or $\jmath_s(h)$, it is usually difficult to acquire the accurate location information of $\wp_s(h)$ in the mapping matrix which, in turn, gives rise to additional challenges in the decoder design. To overcome such a challenge, an index estimator is constructed for the individual case of the descriptions received in the decoder side.

Case I: no packet dropout occurs. In this case, both the description packets $\imath_s(h)$ and $\jmath_s(h)$ are successfully received by the central decoder "$\mathbf{D_C}$", and the index estimation function can be given as

$$\hat{\wp}_s(h) \triangleq \nu_s^c\big(\imath_s(h),\, \jmath_s(h)\big)$$
$$= \begin{cases} 3\imath_s(h) - 2, & \text{if } \imath_s(h) = \jmath_s(h) \\ 3\imath_s(h) - 3, & \text{if } \imath_s(h) = \jmath_s(h) + 1 \text{ and } \imath_s(h) \text{ is odd} \\ 3\imath_s(h), & \text{if } \imath_s(h) = \jmath_s(h) - 1 \text{ and } \imath_s(h) \text{ is odd} \\ 3\imath_s(h) - 4, & \text{if } \imath_s(h) = \jmath_s(h) + 1 \text{ and } \imath_s(h) \text{ is even} \\ 3\imath_s(h) - 1, & \text{if } \imath_s(h) = \jmath_s(h) - 1 \text{ and } \imath_s(h) \text{ is even.} \end{cases} \tag{20}$$

Here, $\nu_s^c(\cdot,\, \cdot)$ denotes the index estimation function and the index estimation error can be calculated as

$$\tilde{\wp}_s(h) \triangleq \hat{\wp}_s(h) - \wp_s(h) = 0. \tag{21}$$

Case II: the packet dropout only occurs in channel "$\mathbf{C_1}$". In this situation, only the description packet $\jmath_s(h)$ is transmitted to the decoder "$\mathbf{D_L}$", and the index estimation function is determined as

$$\hat{\wp}_s(h) \triangleq \nu_s^l\big(\jmath_s(h)\big) = 3\jmath_s(h) - 2. \tag{22}$$

Case III: the packet dropout only occurs in channel "$\mathbf{C_2}$". In this scenario, only the description packet $\imath_s(h)$ is available to the decoder "$\mathbf{D_R}$", and the index estimation function is defined by

$$\hat{\wp}_s(h) \triangleq \nu_s^r\big(\imath_s(h)\big) = 3\imath_s(h) - 2. \tag{23}$$

For **Case II** and **Case III**, we know from (22)-(23) that the index estimation error satisfying

$$\|\tilde{\wp}_s(h)\| \leqslant 2. \tag{24}$$

Case IV: the packet dropout occurs in both channels "$\mathbf{C_1}$" and "$\mathbf{C_2}$". Correspondingly, none of the description packets is accessible at the decoder side and, instead of estimating $\wp_s(h)$, the latest decoded measurement $\vec{y}(h-1)$ is utilized to compensate the value of $\vec{y}(h)$.

Step 2. Decoder Rule Formulation

With the estimated index $\hat{\wp}_s(h)$ in hand, the inverse quantization function can now be developed as follows:

$$\grave{o}_s\big(\hat{\wp}_s(h)\big) \triangleq -r_s + \frac{\big(2\hat{\wp}_s(h) - 1\big)r_s}{l_s}, \quad (s \in \mathfrak{S}). \tag{25}$$

Accordingly, the decoder functions can be determined by

$$\begin{cases} \Re^c\big(\imath(h),\, \jmath(h)\big) = \grave{o}_s\Big(\nu_s^c\big(\imath_s(h),\, \jmath_s(h)\big)\Big) \\ \Re^r\big(\jmath(h)\big) = \grave{o}_s\Big(\nu_s^l\big(\jmath_s(h)\big)\Big) \\ \Re^l\big(\imath(h)\big) = \grave{o}_s\Big(\nu_s^r\big(\imath_s(h)\big)\Big). \end{cases} \tag{26}$$

This article has been accepted for publication in a future issue of this journal, but has not been fully edited. Content may change prior to final publication. Citation information: DOI10.1109/TSMC.2023.3290011 IEEE Transactions on Systems, Man, and Cybernetics: Systems

C. Boundedness Analysis of Decoding Error

In this subsection, we shall focus our attention on the boundedness analysis of decoding error $\kappa(h)$.

Theorem 1: For the encoding procedure (2) and the decoding procedure (3), the decoding error $\kappa(h)$ satisfies

$$\kappa(h) = \begin{cases} \kappa_2(h), \text{ for } \textbf{Case I} & (27a) \\ \kappa_1(h), \text{ for } \textbf{Case II} \text{ and } \textbf{Case III} & (27b) \\ \kappa_0(h), \text{ for } \textbf{Case IV} & (27c) \end{cases}$$

and

$$\begin{cases} \|\kappa_2(h)\| \leqslant \sqrt{\sum_{s=1}^{p_y} \big(\pi_s(h)\big)^2} & (28a) \\ \|\kappa_1(h)\| \leqslant \sqrt{\sum_{s=1}^{p_y} \big(5\pi_s(h)\big)^2} & (28b) \\ \|\kappa_0(h)\| \leqslant \sqrt{\sum_{s=1}^{p_y} \big(\hbar\pi_s(h)\big)^2} & (28c) \end{cases}$$

with $\hbar > 5$ being a bounded positive scalar.

Proof: According to the individual situation of the description packets received at the decoder side, the boundedness of decoding error is analyzed as follows.

For **Case I**, both the description packets $\imath_s(h)$ and $\jmath_s(h)$ are successfully transmitted to the decoder. In this case, keeping in mind the expressions of $\tau_s(h)$ and $\upsilon_s(h)$, we obtain

$$\wp_s(h) = 3\tau_s(h) + \upsilon_s(h), \tag{29}$$

According to (18), (21), (25)-(26), it is not difficult to obtain

$$|\kappa_{2,s}(h)| \leqslant |\pi_s(h)| \tag{30}$$

with $\kappa_{2,s}(h)$ being the sth component of $\kappa_2(h)$. Furthermore, we have

$$\|\kappa_2(h)\| \leqslant \sqrt{\sum_{s=1}^{p_y} \big(\pi_s(h)\big)^2}. \tag{31}$$

For **Case II** and **Case III**, only one description packet ($\imath_s(h)$ or $\jmath_s(h)$) is successfully transmitted to the decoder. Accordingly, it can be concluded from (18), (21), (25)-(26), and (29) that

$$|\kappa_{1,s}(h)| \leqslant 5|\pi_s(h)| \tag{32}$$

where $\kappa_{1,s}(h)$ is the sth component of $\kappa_1(h)$. Similarly, we have

$$\|\kappa_1(h)\| \leqslant \sqrt{\sum_{s=1}^{p_y} \big(5\pi_s(h)\big)^2}. \tag{33}$$

For **Case IV**, no description packet is transmitted to the decoder. Without loss of generality, we assume that the upper bound of $|\kappa_{0,s}(h)|$ is greater than $5|\pi_s(h)|$. In other words, there exists a bounded positive scalar $\hbar > 5$ such that

$$|\kappa_{0,s}(h)| \leqslant \hbar|\pi_s(h)|, \tag{34}$$

which yields

$$\|\kappa_0(h)\| \leqslant \sqrt{\sum_{s=1}^{p_y} \big(\hbar\pi_s(h)\big)^2}. \tag{35}$$

■

D. Boundedness Analysis of Tracking Error

A sufficient condition is derived in the following theorem for assessing the boundedness of tracking error in mean-square sense.

Theorem 2: Let the controller gain matrices P_x, P_χ, I_x, I_χ, D_x and D_χ be given. Assume that there exist positive scalars ω_1, ω_2, ω_3, ω_4, ω_5 and positive definite matrices U, $N^{[\epsilon]}$ ($\epsilon = 1, 2, \ldots, q$) such that the following inequality holds:

$$\Delta_1 = \begin{bmatrix} \Delta_1^{[1]} & \star \\ \Delta_1^{[2]} & \Delta_1^{[3]} \end{bmatrix} < 0 \tag{36}$$

where

$$\begin{aligned} \Delta_1^{[1]} &\triangleq \text{diag}\{\Delta_1^{[4]},\ -N,\ -\omega_2\mathbf{I},\ -\omega_3\mathbf{I},\ -\omega_4\mathbf{I},\ -\omega_5\mathbf{I}\} \\ \Delta_1^{[2]} &\triangleq \big[\mathcal{A} \quad \mathcal{S} \quad \mathcal{W} \quad \mathcal{T}\hat{\Xi}_0 \quad \mathcal{T}\hat{\Xi}_1 \quad \mathcal{T}\hat{\Xi}_2\big] \\ \Delta_1^{[3]} &\triangleq -U^{-1}, \quad \Delta_1^{[4]} \triangleq -U + \omega_1 U + \sum_{\epsilon=1}^{q} N^{[\epsilon]} \\ N &\triangleq \text{diag}\{N^{[1]}, \quad N^{[2]}, \quad \cdots, \quad N^{[q]}\}. \end{aligned}$$

Then, the output tracking error dynamics $z_\varepsilon(h)$ is EUBMS. Correspondingly, the AUB of $\|z_\varepsilon(h)\|^2$ is given by

$$\begin{aligned} \theta_3 =& \Bigg((\hbar^2\breve{\omega}_3 + 25\breve{\omega}_4 + \breve{\omega}_5)(q+1) \sum_{s=1}^{p_y} \frac{\varpi_s^2 r_s^2}{l_s^2} \\ &+ \omega_2(\bar{v}^2 + \bar{\mu}^2) \Bigg) \frac{\lambda_{\max}(\mathcal{E}^T\mathcal{E})\rho_3}{\lambda_-^{[UN]}(\rho_3 - 1)} \end{aligned} \tag{37}$$

with

$$\begin{aligned} \breve{\omega}_3 &\triangleq \omega_3 + \bar{\xi}_0 - \bar{\xi}_0^2, \quad \lambda_-^{[U]} \triangleq \lambda_{\min}(U) \\ \breve{\omega}_4 &\triangleq \omega_4 + \bar{\xi}_1 - \bar{\xi}_1^2, \quad \lambda_-^{[N]} \triangleq \lambda_{\min}(N) \\ \breve{\omega}_5 &\triangleq \omega_5 + \bar{\xi}_2 - \bar{\xi}_2^2, \quad \lambda_-^{[UN]} \triangleq \min\{\lambda_-^{[U]},\ \lambda_-^{[N]}\}. \end{aligned}$$

In addition, the constant $\rho_3 > 1$ in (37) can be obtained according to

$$\lambda_+^{[U]}(\rho_3 - 1 - \rho_3\omega_1) + \lambda_+^{[N]}(\rho_3 - 1)q^2\rho_1^q = 0 \tag{38}$$

where

$$\lambda_+^{[U]} \triangleq \lambda_{\max}(U), \quad \lambda_+^{[N]} \triangleq \lambda_{\max}(N).$$

Proof: Construct the following Lyapunov-like functional:

$$V\big(\flat(h)\big) = V_1\big(\flat(h)\big) + V_2\big(\flat(h)\big) \tag{39}$$

with

$$\begin{aligned} V_1\big(\flat(h)\big) &\triangleq \flat^T(h) U \flat(h) \\ V_2\big(\flat(h)\big) &\triangleq \sum_{\epsilon=1}^{q} \sum_{\ell=h-\epsilon}^{h-1} \flat^T(\ell) N^{[\epsilon]} \flat(\ell). \end{aligned}$$

The difference of $V\big(\flat(h)\big)$ is expressed as

$$\natural V\big(\flat(h)\big)=\sum_{i=1}^{2}\natural V_i\big(\flat(h)\big) \tag{40}$$

with

$$\begin{aligned}\natural V_1\big(\flat(h)\big) &\triangleq\mathbb{E}\{V_1\big(\flat(h+1)\big)|\flat(h)\}-V_1\big(\flat(h)\big)\\ \natural V_2\big(\flat(h)\big) &\triangleq\mathbb{E}\{V_2\big(\flat(h+1)\big)|\flat(h)\}-V_2\big(\flat(h)\big).\end{aligned}$$

Calculating $\natural_i V(h)$ $(i=1,\,2)$ and taking the mathematical expectation along the trajectory of (12), we have

$$\begin{aligned}&\mathbb{E}\left\{\natural V_1\big(\flat(h)\big)\right\}\\ =&\mathbb{E}\left\{V_1\big(\flat(h+1)\big)-V_1\big(\flat(h)\big)\right\}\\ =&\mathbb{E}\Big\{\Big(\mathcal{A}\flat(h)+\mathcal{S}\varrho(h)+\mathcal{W}o(h)+\mathcal{T}\big(\hat{\Xi}_0+\tilde{\Xi}_0(h)\big)\iota_0(h)\\ &+\mathcal{T}\big(\hat{\Xi}_1+\tilde{\Xi}_1(h)\big)\iota_1(h)+\mathcal{T}\big(\hat{\Xi}_2+\tilde{\Xi}_2(h)\big)\iota_2(h)\Big)^TU\\ &\times\Big(\mathcal{A}\flat(h)+\mathcal{S}\varrho(h)+\mathcal{W}o(h)+\mathcal{T}\big(\hat{\Xi}_0+\tilde{\Xi}_0(h)\big)\iota_0(h)\\ &+\mathcal{T}\big(\hat{\Xi}_1+\tilde{\Xi}_1(h)\big)\iota_1(h)+\mathcal{T}\big(\hat{\Xi}_2+\tilde{\Xi}_2(h)\big)\iota_2(h)\Big)\\ &-\flat^T(h)U\flat(h)\Big\}\\ =&\mathbb{E}\Big\{\flat^T(h)(\mathcal{A}^TU\mathcal{A}-U+\omega_1\mathbf{I})\flat(h)+\varrho^T(h)\mathcal{S}^TU\mathcal{S}\varrho(h)\\ &+o^T(h)(\mathcal{W}^TU\mathcal{W}-\omega_2\mathbf{I})o(h)+\iota_0^T(h)(\hat{\Xi}_0^2\mathcal{T}^TU\mathcal{T}-\omega_3\mathbf{I})\\ &\times\iota_0(h)+\iota_1^T(h)(\hat{\Xi}_1^2\mathcal{T}^TU\mathcal{T}-\omega_4\mathbf{I})\iota_1(h)+\iota_2^T(h)(\hat{\Xi}_2^2\mathcal{T}^T\\ &\times U\mathcal{T}-\omega_5\mathbf{I})\iota_2(h)+2\varrho^T(h)\mathcal{S}^TU\mathcal{A}\flat(h)+2o^T(h)\mathcal{W}^T\\ &\times U\mathcal{A}\flat(h)+2o^T(h)\mathcal{W}^TU\mathcal{S}\varrho(h)+2\iota_0^T(h)\hat{\Xi}_0\mathcal{T}^TU\mathcal{A}\flat(h)\\ &+2\iota_0^T(h)\hat{\Xi}_0\mathcal{T}^TU\mathcal{S}\varrho(h)+2\iota_0^T(h)\hat{\Xi}_0\mathcal{T}^TU\mathcal{W}o(h)\\ &+2\iota_1^T(h)\hat{\Xi}_1\mathcal{T}^TU\mathcal{A}\flat(h)+2\iota_1^T(h)\hat{\Xi}_1\mathcal{T}^TU\mathcal{S}\varrho(h)\\ &+2\iota_1^T(h)\hat{\Xi}_1\mathcal{T}^TU\mathcal{W}o(h)+2\iota_2^T(h)\hat{\Xi}_2\mathcal{T}^TU\mathcal{A}\flat(h)\\ &+2\iota_2^T(h)\hat{\Xi}_2\mathcal{T}^TU\mathcal{S}\varrho(h)+2\iota_2^T(h)\hat{\Xi}_2\mathcal{T}^TU\mathcal{W}o(h)\\ &+2\iota_1^T(h)\hat{\Xi}_1\hat{\Xi}_0\mathcal{T}^TU\mathcal{T}\iota_0(h)+2\iota_2^T(h)\hat{\Xi}_2\hat{\Xi}_0\mathcal{T}^TU\mathcal{T}\iota_0(h)\\ &+2\iota_2^T(h)\hat{\Xi}_2\hat{\Xi}_1\mathcal{T}^TU\mathcal{T}\iota_1(h)-\omega_1V_1\big(\flat(h)\big)\\ &+\omega_2o^T(h)o(h)+\breve{\omega}_3\iota_0^T(h)\iota_0(h)+\breve{\omega}_4\iota_1^T(h)\iota_1(h)\\ &+\breve{\omega}_5\iota_2^T(h)\iota_2(h)\Big\}\end{aligned} \tag{41}$$

and

$$\begin{aligned}&\mathbb{E}\left\{\natural V_2\big(\flat(h)\big)\right\}\\ =&\mathbb{E}\left\{V_2\big(\flat(h+1)\big)-V_2\big(\flat(h)\big)\right\}\\ =&\mathbb{E}\left\{\sum_{\epsilon=1}^{q}\left(\sum_{\ell=h+1-\epsilon}^{h}\flat^T(\ell)N^{[\epsilon]}\flat(\ell)-\sum_{\ell=h-\epsilon}^{h-1}\flat^T(\ell)N^{[\epsilon]}\flat(\ell)\right)\right\}\\ =&\sum_{\epsilon=1}^{q}\mathbb{E}\left\{\flat^T(h)N^{[\epsilon]}\flat(h)-\flat^T(h-\epsilon)N^{[\epsilon]}\flat(h-\epsilon)\right\}.\end{aligned} \tag{42}$$

Denoting

$$\Im(h)\triangleq\begin{bmatrix}\flat^T(h) & \varrho^T(h) & o^T(h) & \iota_0^T(h) & \iota_1^T(h) & \iota_2^T(h)\end{bmatrix}^T$$

and substituting (41)-(42) into (40) lead to

$$\begin{aligned}&\mathbb{E}\left\{\natural V\big(\flat(h)\big)\right\}\\ =&\mathbb{E}\left\{\Im^T(h)\Theta_1\Im(h)\right\}-\omega_1\mathbb{E}\left\{V_1\big(\flat(h)\big)\right\}\\ &+\omega_2o^T(h)o(h)+\breve{\omega}_3\iota_0^T(h)\iota_0(h)\\ &+\breve{\omega}_4\iota_1^T(h)\iota_1(h)+\breve{\omega}_5\iota_2^T(h)\iota_2(h)\end{aligned} \tag{43}$$

where

$$\Theta_1\triangleq\begin{bmatrix}\Theta_1^{[11]} & \star & \star & \star & \star & \star\\ \Theta_1^{[21]} & \Theta_1^{[22]} & \star & \star & \star & \star\\ \Theta_1^{[31]} & \Theta_1^{[32]} & \Theta_1^{[33]} & \star & \star & \star\\ \Theta_1^{[41]} & \Theta_1^{[42]} & \Theta_1^{[43]} & \Theta_1^{[44]} & \star & \star\\ \Theta_1^{[51]} & \Theta_1^{[52]} & \Theta_1^{[53]} & \Theta_1^{[54]} & \Theta_1^{[55]} & \star\\ \Theta_1^{[61]} & \Theta_1^{[62]} & \Theta_1^{[63]} & \Theta_1^{[64]} & \Theta_1^{[65]} & \Theta_1^{[66]}\end{bmatrix}$$

$$\begin{aligned}&\Theta_1^{[11]}\triangleq\mathcal{A}^TU\mathcal{A}-U+\omega_1U+\sum_{\epsilon=1}^{q}N^{[\epsilon]}\\ &\Theta_1^{[22]}\triangleq-N+\mathcal{S}^TU\mathcal{S}, && \Theta_1^{[33]}\triangleq\mathcal{W}^TU\mathcal{W}-\omega_2\mathbf{I}\\ &\Theta_1^{[44]}\triangleq\hat{\Xi}_0^2\mathcal{T}^TU\mathcal{T}-\omega_3\mathbf{I}, && \Theta_1^{[55]}\triangleq\hat{\Xi}_1^2\mathcal{T}^TU\mathcal{T}-\omega_4\mathbf{I}\\ &\Theta_1^{[66]}\triangleq\hat{\Xi}_2^2\mathcal{T}^TU\mathcal{T}-\omega_5\mathbf{I}, && \Theta_1^{[21]}\triangleq\mathcal{S}^TU\mathcal{A}\\ &\Theta_1^{[31]}\triangleq\mathcal{W}^TU\mathcal{A}, && \Theta_1^{[32]}\triangleq\mathcal{W}^TU\mathcal{S}\\ &\Theta_1^{[41]}\triangleq\hat{\Xi}_0\mathcal{T}^TU\mathcal{A}, && \Theta_1^{[42]}\triangleq\hat{\Xi}_0\mathcal{T}^TU\mathcal{S}\\ &\Theta_1^{[43]}\triangleq\hat{\Xi}_0\mathcal{T}^TU\mathcal{W}, && \Theta_1^{[51]}\triangleq\hat{\Xi}_1\mathcal{T}^TU\mathcal{A}\\ &\Theta_1^{[52]}\triangleq\hat{\Xi}_1\mathcal{T}^TU\mathcal{S}, && \Theta_1^{[53]}\triangleq\hat{\Xi}_1\mathcal{T}^TU\mathcal{W}\\ &\Theta_1^{[54]}\triangleq\hat{\Xi}_1\hat{\Xi}_0\mathcal{T}^TU\mathcal{T}, && \Theta_1^{[61]}\triangleq\hat{\Xi}_2\mathcal{T}^TU\mathcal{A}\\ &\Theta_1^{[62]}\triangleq\hat{\Xi}_2\mathcal{T}^TU\mathcal{S}, && \Theta_1^{[63]}\triangleq\hat{\Xi}_2\mathcal{T}^TU\mathcal{W}\\ &\Theta_1^{[64]}\triangleq\hat{\Xi}_2\hat{\Xi}_0\mathcal{T}^TU\mathcal{T}, && \Theta_1^{[65]}\triangleq\hat{\Xi}_2\hat{\Xi}_1\mathcal{T}^TU\mathcal{T}.\end{aligned}$$

Furthermore, it follows easily from the Schur Complement Lemma that $\Theta_1<0$ is ensured by condition (36), which implies that

$$\begin{aligned}&\mathbb{E}\left\{\natural V\big(\flat(h)\big)\right\}\\ <&-\omega_1\mathbb{E}\left\{V_1\big(\flat(h)\big)\right\}+\omega_2o^T(h)o(h)+\breve{\omega}_3\iota_0^T(h)\iota_0(h)\\ &+\breve{\omega}_4\iota_1^T(h)\iota_1(h)+\breve{\omega}_5\iota_2^T(h)\iota_2(h).\end{aligned} \tag{44}$$

Letting

$$\begin{aligned}\theta_3^{[1]}(h)\triangleq&\omega_2o^T(h)o(h)+\breve{\omega}_3\iota_0^T(h)\iota_0(h)\\ &+\breve{\omega}_4\iota_1^T(h)\iota_1(h)+\breve{\omega}_5\iota_2^T(h)\iota_2(h)\end{aligned}$$

and recalling the expressions of $o(h)$, $\iota_0(h)$, $\iota_1(h)$, $\iota_0(h)$, we have from (17), (27a)-(27c) and (28a)-(28c) that

$$\begin{aligned}&\theta_3^{[1]}(h)\\ \leqslant&(\hbar^2\breve{\omega}_3+25\breve{\omega}_4+\breve{\omega}_5)(q+1)\sum_{s=1}^{p_y}\frac{\varpi_s^2r_s^2}{l_s^2}\\ &+\omega_2(\bar{v}^2+\bar{\mu}^2)\triangleq\theta_3^{[2]}\end{aligned} \tag{45}$$

and

$$\mathbb{E}\left\{\natural V\big(\flat(h)\big)\right\}<-\omega_1\mathbb{E}\left\{V_1\big(\flat(h)\big)\right\}+\theta_3^{[2]}. \tag{46}$$

For any positive scalar $\rho_1>1$, it follows that

$$\begin{aligned}&\mathbb{E}\left\{\rho_1^{h+1}V\big(\flat(h+1)\big)\right\}-\mathbb{E}\left\{\rho_1^{h}V\big(\flat(h)\big)\right\}\\ =&\rho_1^{h+1}\mathbb{E}\left\{\natural V\big(\flat(h)\big)\right\}+\rho_1^{h}(\rho_1-1)\mathbb{E}\left\{V\big(\flat(h)\big)\right\}\\ <&\rho_1^{h+1}\Big(-\omega_1\mathbb{E}\big\{V_1\big(\flat(h)\big)\big\}+\theta_3^{[2]}\Big)\end{aligned}$$

This article has been accepted for publication in a future issue of this journal, but has not been fully edited. Content may change prior to final publication. Citation information: DOI10.1109/TSMC.2023.3290011 IEEE Transactions on Systems, Man, and Cybernetics: Systems

$$
\begin{aligned}
&+ \rho_1^h(\rho_1 - 1)\mathbb{E}\left\{V\big(\flat(h)\big)\right\} \\
\leqslant& \gamma_1(\rho_1)\rho_1^h\mathbb{E}\left\{\|\flat(h)\|^2\right\} + \rho_1^{h+1}\theta_3^{[2]} \\
&+ \gamma_2(\rho_1)\sum_{\epsilon=h-q}^{h-1}\rho_1^h\mathbb{E}\{\|\flat(\epsilon)\|^2\}
\end{aligned} \tag{47}
$$

with

$$
\begin{aligned}
\gamma_1(\rho_1) \triangleq& \lambda_+^{[U]}(\rho_1 - 1 - \rho_1\omega_1) \\
\gamma_2(\rho_1) \triangleq& \lambda_+^{[N]}q(\rho_1 - 1).
\end{aligned}
$$

Next, for any integer $\rho_2 \geqslant q+1$, by taking cumulative summation for both sides of (47) from 0 to $\rho_2 - 1$ with respect to h, we have

$$
\begin{aligned}
&\rho_1^{\rho_2}\mathbb{E}\left\{V\big(\flat(\rho_2)\big)\right\} - \mathbb{E}\left\{V\big(\flat(0)\big)\right\} \\
<& \gamma_1(\rho_1)\sum_{h=0}^{\rho_2-1}\rho_1^h\mathbb{E}\left\{\|\flat(h)\|^2\right\} + \frac{\rho_1(1-\rho_1^{\rho_2})}{1-\rho_1}\theta_3^{[2]} \\
&+ \gamma_2(\rho_1)\sum_{h=0}^{\rho_2-1}\sum_{\epsilon=h-q}^{h-1}\rho_1^h\mathbb{E}\{\|\flat(\epsilon)\|^2\}.
\end{aligned} \tag{48}
$$

Calculating the last term on the right-hand side of (48) yields

$$
\begin{aligned}
&\sum_{h=0}^{\rho_2-1}\sum_{\epsilon=h-q}^{h-1}\rho_1^h\mathbb{E}\{\|\flat(\epsilon)\|^2\} \\
\leqslant& \left(\sum_{\epsilon=-q}^{-1}\sum_{h=0}^{\epsilon+q} + \sum_{\epsilon=0}^{\rho_2-q-1}\sum_{h=\epsilon+1}^{\epsilon+q} + \sum_{\epsilon=\rho_2-q}^{\rho_2-1}\sum_{h=\epsilon+1}^{\rho_2-1}\right)\rho_1^h\mathbb{E}\{\|\flat(\epsilon)\|^2\} \\
\leqslant& q\sum_{\epsilon=-q}^{-1}\rho_1^{\epsilon+q}\mathbb{E}\{\|\flat(\epsilon)\|^2\} + q\sum_{\epsilon=0}^{\rho_2-q-1}\rho_1^{\epsilon+q}\mathbb{E}\{\|\flat(\epsilon)\|^2\} \\
&+ q\sum_{\epsilon=\rho_2-q}^{\rho_2-1}\rho_1^{\epsilon+q}\mathbb{E}\{\|\flat(\epsilon)\|^2\} \\
\leqslant& q\rho_1^q\sup_{\ell\in[-q,\,0]}\mathbb{E}\{\|\flat(\ell)\|^2\} + q\rho_1^q\sum_{\epsilon=0}^{\rho_2-1}\rho_1^{\epsilon}\mathbb{E}\{\|\flat(\epsilon)\|^2\},
\end{aligned} \tag{49}
$$

which, together with (48), gives

$$
\begin{aligned}
&\rho_1^{\rho_2}\mathbb{E}\left\{V\big(\flat(\rho_2)\big)\right\} - \mathbb{E}\left\{V\big(\flat(0)\big)\right\} \\
<& \gamma_3(\rho_1)\sum_{h=0}^{\rho_2-1}\rho_1^h\mathbb{E}\left\{\|\flat(h)\|^2\right\} + \frac{\rho_1(1-\rho_1^{\rho_2})}{1-\rho_1}\theta_3^{[2]} \\
&+ \gamma_4(\rho_1)\sup_{\ell\in[-q,\,0]}\mathbb{E}\{\|\flat(\ell)\|^2\}
\end{aligned} \tag{50}
$$

with

$$
\gamma_3(\rho_1) \triangleq \gamma_1(\rho_1) + \gamma_2(\rho_1)q\rho_1^q, \quad \gamma_4(\rho_1) \triangleq \gamma_2(\rho_1)q\rho_1^q.
$$

Keeping in mind $\gamma_3(1) = -\omega_1\lambda_+^{[U]} < 0$ and $\lim_{\rho_1\to\infty}\gamma_3(\rho_1) = +\infty$, it is easy to see that there exists a scalar $\rho_3 > 1$ such that $\gamma_3(\rho_3) = 0$, which indicates

$$
\begin{aligned}
&\rho_3^{\rho_2}\mathbb{E}\left\{V\big(\flat(\rho_2)\big)\right\} - \mathbb{E}\left\{V\big(\flat(0)\big)\right\} \\
<& \gamma_4(\rho_3)\sup_{\ell\in[-q,\,0]}\mathbb{E}\{\|\flat(\ell)\|^2\} + \frac{\rho_3(1-\rho_3^{\rho_2})}{1-\rho_3}\theta_3^{[2]}.
\end{aligned} \tag{51}
$$

In terms of the definition of $V\big(\flat(h)\big)$, we have

$$
\mathbb{E}\left\{V\big(\flat(\rho_2)\big)\right\} \geqslant \lambda_-^{[UN]}\mathbb{E}\{\|\flat(\rho_2)\|^2\} \tag{52}
$$

and

$$
\mathbb{E}\left\{V\big(\flat(0)\big)\right\} \leqslant \lambda_+^{[UN]}\sup_{\ell\in[-q,\,0]}\mathbb{E}\{\|\flat(\ell)\|^2\} \tag{53}
$$

with

$$
\lambda_+^{[UN]} \triangleq \max\{\lambda_+^{[U]},\, \lambda_+^{[N]}\},
$$

which results in

$$
\begin{aligned}
&\mathbb{E}\{\|\flat(\rho_2)\|^2\} \\
<& \frac{\lambda_+^{[UN]} + \gamma_4(\rho_3)}{\lambda_-^{[UN]}\rho_3^{\rho_2}}\sup_{\ell\in[-q,\,0]}\mathbb{E}\{\|\flat(\ell)\|^2\} \\
&+ \frac{\rho_3(1-\rho_3^{\rho_2})}{\lambda_-^{[UN]}\rho_3^{\rho_2}(1-\rho_3)}\theta_3^{[2]}.
\end{aligned} \tag{54}
$$

Based on the expression of $z_\varepsilon(h)$, we now conclude that

$$
\begin{aligned}
&\mathbb{E}\{\|z_\varepsilon(h)\|^2\} \\
<& \frac{\lambda_+^{[UN]} + \gamma_4(\rho_3)}{\lambda_-^{[UN]}\rho_3^h}\lambda_{\max}(\mathcal{E}^T\mathcal{E})\sup_{\ell\in[-q,\,0]}\mathbb{E}\{\|\flat(\ell)\|^2\} \\
&+ \frac{\rho_3(1-\rho_3^h)}{\lambda_-^{[UN]}\rho_3^h(1-\rho_3)}\lambda_{\max}(\mathcal{E}^T\mathcal{E})\theta_3^{[2]}.
\end{aligned} \tag{55}
$$

Subsequently, letting

$$
\begin{aligned}
\theta_1 \triangleq& \rho_3^{-1} \\
\theta_2 \triangleq& \frac{\lambda_+^{[UN]} + \gamma_4(\rho_3)}{\lambda_-^{[UN]}}\lambda_{\max}(\mathcal{E}^T\mathcal{E})\sup_{\ell\in[-q,\,0]}\mathbb{E}\{\|\flat(\ell)\|^2\} \\
\theta_3^{[3]}(h) \triangleq& \frac{\rho_3(1-\rho_3^h)}{\lambda_-^{[UN]}\rho_3^h(1-\rho_3)}\lambda_{\max}(\mathcal{E}^T\mathcal{E})\theta_3^{[2]}
\end{aligned}
$$

and calculating the limit of $\theta_3^{[3]}(h)$ with respect to h approaches to $+\infty$, one has

$$
\mathbb{E}\{\|z_\varepsilon(h)\|^2\} < \theta_1^h\theta_2 + \theta_3 \tag{56}
$$

where

$$
\theta_3 \triangleq \lim_{h\to+\infty}\theta_3^{[3]}(h) = \frac{\lambda_{\max}(\mathcal{E}^T\mathcal{E})\theta_3^{[2]}\rho_3}{\lambda_-^{[UN]}(\rho_3 - 1)}.
$$

According to (13) and (56), it is easy to draw the conclusion that the output tracking error dynamics $z_\varepsilon(h)$ is EUBMS, which completes the proof. ■

E. Design of PID Controller

In the following theorem, the PID controller parameters are designed to minimize the AUB of $\|z_\varepsilon(h)\|^2$.

Theorem 3: Let the positive scalar ω_1 be given. Assume that there exist positive scalars ω_2, ω_3, ω_4, ω_5, positive definite matrices $U_{[1]}$, $U_{[2]}$, $N^{[\epsilon]}$ ($\epsilon = 1, 2, \ldots, q$) and matrices $Y_{[1]}$, $Y_{[2]}$, $Y_{[3]}$, $\breve{P}_x$, $\breve{P}_\chi$, $\breve{I}_x$, $\breve{I}_\chi$, $\breve{D}_x$ $\breve{D}_\chi$ such that the following inequality holds:

$$
\Delta_2 = \begin{bmatrix} \Delta_1^{[1]} & \star \\ \Delta_2^{[2]} & \Delta_2^{[3]} \end{bmatrix} < 0 \tag{57}
$$

This article has been accepted for publication in a future issue of this journal, but has not been fully edited. Content may change prior to final publication. Citation information: DOI10.1109/TSMC.2023.3290011 IEEE Transactions on Systems, Man, and Cybernetics: Systems

where

$$\begin{aligned}
&\Delta_2^{[2]} \triangleq \begin{bmatrix}\breve{\mathcal{A}} & \breve{\mathcal{S}} & \breve{\mathcal{W}} & \breve{\mathcal{T}}\hat{\Xi}_0 & \breve{\mathcal{T}}\hat{\Xi}_1 & \breve{\mathcal{T}}\hat{\Xi}_2\end{bmatrix}\\
&\Delta_2^{[3]} \triangleq \mathrm{diag}\{U_{[1]} - Y_{[\Upsilon]} - Y_{[\Upsilon]}^T, -U_{[2]}\}, U \triangleq \mathrm{diag}\{U_{[1]}, U_{[2]}\}\\
&\quad \Upsilon \triangleq [B(B^TB)^{-1} \quad (B^T)^{\perp}]^T, \quad Y \triangleq \begin{bmatrix} Y_{[1]} & Y_{[2]} \\ \mathbf{0} & Y_{[3]}\end{bmatrix}\\
&\quad \breve{\mathcal{A}} \triangleq \breve{\mathscr{A}} + \breve{\mathscr{B}},\ \breve{\mathcal{S}} \triangleq \begin{bmatrix}\breve{\mathscr{R}}_1\mathscr{C} \\ \mathbf{0}\end{bmatrix},\ \breve{\mathcal{T}} \triangleq \begin{bmatrix}\breve{\mathscr{R}}_2 \\ \mathbf{0}\end{bmatrix},\ Y_{[\Upsilon]} \triangleq Y\Upsilon\\
&\quad \breve{\mathcal{W}} \triangleq \begin{bmatrix} Y_{[\Upsilon]}M & -Y_{[\Upsilon]}G \\ \mathbf{0} & U_{[2]}G\end{bmatrix}, \quad \breve{\mathscr{A}} \triangleq \begin{bmatrix} Y_{[\Upsilon]}A & Y_{[\Upsilon]}(A-F) \\ \mathbf{0} & U_{[2]}F\end{bmatrix}\\
&\quad \breve{\mathscr{B}} \triangleq \begin{bmatrix}(P_x^{[\Upsilon]} + D_x^{[\Upsilon]})C & (P_\chi^{[\Upsilon]} + D_\chi^{[\Upsilon]})(C+H) \\ \mathbf{0} & \mathbf{0}\end{bmatrix}\\
&\quad \breve{\mathscr{R}}_1 \triangleq [\breve{\mathscr{I}} + \breve{\mathscr{D}} \quad \underbrace{\breve{\mathscr{I}} \ \cdots \ \breve{\mathscr{I}}}_{q-1}], \quad \breve{\mathscr{I}} \triangleq \begin{bmatrix} I_x^{[\Upsilon]} & I_\chi^{[\Upsilon]}\end{bmatrix}\\
&\quad \breve{\mathscr{R}}_2 \triangleq [P_x^{[\Upsilon]} + D_x^{[\Upsilon]} \quad I_x^{[\Upsilon]} + D_x^{[\Upsilon]} \quad \underbrace{I_x^{[\Upsilon]} \ \cdots \ I_x^{[\Upsilon]}}_{q-1}]\\
&\quad \breve{\mathscr{D}} \triangleq \begin{bmatrix} D_x^{[\Upsilon]} & D_\chi^{[\Upsilon]}\end{bmatrix}, \quad P_x^{[\Upsilon]} \triangleq \begin{bmatrix}\breve{P}_x \\ \mathbf{0}\end{bmatrix}, \quad I_x^{[\Upsilon]} \triangleq \begin{bmatrix}\breve{I}_x \\ \mathbf{0}\end{bmatrix}\\
&D_x^{[\Upsilon]} \triangleq \begin{bmatrix}\breve{D}_x \\ \mathbf{0}\end{bmatrix},\ P_\chi^{[\Upsilon]} \triangleq \begin{bmatrix}\breve{P}_\chi \\ \mathbf{0}\end{bmatrix},\ I_\chi^{[\Upsilon]} \triangleq \begin{bmatrix}\breve{I}_\chi \\ \mathbf{0}\end{bmatrix},\ D_\chi^{[\Upsilon]} \triangleq \begin{bmatrix}\breve{D}_\chi \\ \mathbf{0}\end{bmatrix}.
\end{aligned}$$

Then, the output tracking error dynamics $z_\varepsilon(h)$ is EUBMS. Additionally, the minimum of the AUB of $\|z_\varepsilon(h)\|^2$ can be obtained by solving the following minimization problem:

$$\begin{aligned}
&\min \quad (\hbar^2\breve{\omega}_3 + 25\breve{\omega}_4 + \breve{\omega}_5)(q+1)\sum_{s=1}^{p_y}\frac{\varpi_s^2 r_s^2}{l_s^2} + \omega_2(\bar{v}^2 + \bar{\mu}^2)\\
&\qquad \text{subject to} \quad (57).
\end{aligned} \tag{58}$$

Correspondingly, the desired controller gain matrices are given by

$$\begin{aligned}
P_x &= Y_{[1]}^{-1}\breve{P}_x, \quad P_\chi = Y_{[1]}^{-1}\breve{P}_\chi\\
I_x &= Y_{[1]}^{-1}\breve{I}_x, \quad I_\chi = Y_{[1]}^{-1}\breve{I}_\chi\\
D_x &= Y_{[1]}^{-1}\breve{D}_x, \quad D_\chi = Y_{[1]}^{-1}\breve{D}_\chi.
\end{aligned} \tag{59}$$

Proof: Performing the congruence transformation to (36) by diag$\{\mathbf{I}, \mathbf{I}, \mathbf{I}, \mathbf{I}, \mathbf{I}, \mathbf{I}, U_{[Y]}\}$ yields

$$\Delta_3 = \begin{bmatrix}\Delta_1^{[1]} & \star \\ \Delta_3^{[2]} & \Delta_3^{[3]}\end{bmatrix} < 0 \tag{60}$$

where

$$\begin{aligned}
&\Delta_3^{[2]} \triangleq \begin{bmatrix}\acute{\mathcal{A}} & \acute{\mathcal{S}} & \breve{\mathcal{W}} & \acute{\mathcal{T}}\hat{\Xi}_0 & \acute{\mathcal{T}}\hat{\Xi}_1 & \acute{\mathcal{T}}\hat{\Xi}_2\end{bmatrix}\\
&\Delta_3^{[3]} \triangleq \mathrm{diag}\{Y_{[\Upsilon]}U_{[1]}^{-1}Y_{[\Upsilon]}^T, -U_{[2]}\}, \quad U_{[Y]} \triangleq \mathrm{diag}\{Y_{[\Upsilon]}, U_{[2]}\}\\
&\quad \acute{\mathcal{A}} \triangleq \breve{\mathscr{A}} + \acute{\mathscr{B}}, \quad \acute{\mathcal{S}} \triangleq \begin{bmatrix} Y_{[\Upsilon]}B\mathscr{R}_1\mathscr{C} \\ \mathbf{0}\end{bmatrix}, \quad \acute{\mathcal{T}} \triangleq \begin{bmatrix} Y_{[\Upsilon]}B\mathscr{R}_2 \\ \mathbf{0}\end{bmatrix}\\
&\quad \acute{\mathscr{B}} \triangleq \begin{bmatrix} Y_{[\Upsilon]}B(P_x + D_x)C & Y_{[\Upsilon]}B(P_\chi + D_\chi)(C+H) \\ \mathbf{0} & \mathbf{0}\end{bmatrix}.
\end{aligned}$$

Bearing in mind the fact that

$$\begin{aligned}
&Y_{[\Upsilon]} + Y_{[\Upsilon]}^T - Y_{[\Upsilon]}U_{[1]}^{-1}Y_{[\Upsilon]}^T - U_{[1]}\\
&= -(Y_{[\Upsilon]} - U_{[1]})U_{[1]}^{-1}(Y_{[\Upsilon]} - U_{[1]})^T \leqslant 0,
\end{aligned} \tag{61}$$

we obtain

$$-Y_{[\Upsilon]}U_{[1]}^{-1}Y_{[\Upsilon]}^T \leqslant U_{[1]} - Y_{[\Upsilon]} - Y_{[\Upsilon]}^T. \tag{62}$$

Putting

$$\begin{aligned}
\breve{P}_x &= Y_{[1]}P_x, \quad \breve{P}_\chi = Y_{[1]}P_\chi\\
\breve{P}_x &= Y_{[1]}I_x, \quad \breve{P}_\chi = Y_{[1]}I_\chi\\
\breve{P}_x &= Y_{[1]}D_x, \quad \breve{P}_\chi = Y_{[1]}D_\chi
\end{aligned} \tag{63}$$

into (60) and recalling (62), we know that (60) can be ensured by condition (57). Thus, according to (13), the output tracking error dynamics $z_\varepsilon(h)$ is EUBMS.

Paying attention to (56), it is easy to find that

$$\begin{aligned}
&\mathbb{E}\{\|z_\varepsilon(h)\|^2\}\\
&< \frac{1}{\rho_3^h}\left(\frac{\lambda_+^{[UN]} + \gamma_4(\rho_3)}{\lambda_-^{[UN]}}\lambda_{\max}(\mathcal{E}^T\mathcal{E})\sup_{\ell\in[-q,0]}\mathbb{E}\{\|\flat(\ell)\|^2\}\right)\\
&\quad + \Bigg((\hbar^2\breve{\omega}_3 + 25\breve{\omega}_4 + \breve{\omega}_5)(q+1)\sum_{s=1}^{p_y}\frac{\varpi_s^2 r_s^2}{l_s^2}\\
&\quad + \omega_2(\bar{v}^2 + \bar{\mu}^2)\Bigg)\frac{\lambda_{\max}(\mathcal{E}^T\mathcal{E})\rho_3}{\lambda_-^{[UN]}(\rho_3 - 1)}.
\end{aligned} \tag{64}$$

Accordingly, we can obtain the minimum of the AUB of $\|z_\varepsilon(h)\|^2$ by solving the minimization problem (58), which completes the proof. ■

Remark 4: Hitherto, Theorem 1 discusses the boundedness of decoding error $\kappa(h)$. Subsequently, Theorem 2 analyzes the ultimate boundedness of the output tracking error dynamics $z_\varepsilon(h)$ in the mean-square sense. Theorem 3 provides the explicit parameterization of the PID controller gains that fulfill the requirement of minimizing the AUB of $\|z_\varepsilon(h)\|^2$. It is revealed that the minimized upper bound of $\|z_\varepsilon(h)\|^2$ is related to important system parameters including the decoding error, the exogenous disturbance upper bound $\bar{v}$ and the reference input upper bound $\bar{\mu}$. In particular, when $\bar{v}$ and $\bar{\mu}$ are fixed, a larger decoding error would lead to a larger upper bound of $\|z_\varepsilon(h)\|^2$ and, accordingly, a larger tracking error, which means a deterioration of the tracking performance.

Remark 5: Up to now, we have endeavored to solve the PID tracking control problem for a class of linear discrete-time systems subject to bounded disturbance input, bounded reference input and ROPD under the MDEM. Pertaining to the rich literature on traditional PID control, the main results presented in this paper own the following specific characteristics: 1) the addressed PID tracking control problem is novel since both the ROPD and MDEM are taken into serious account; 2) the developed MDEM is suitable for enhancing the transmission reliability in the presence of ROPDs; and 3) the established theoretical framework enables the qualitative assessment of the impact from the decoding error on the tracking accuracy.

F. Design of P-Type Controller

In this subsection, for comparison purposes, let us deal with the special case of constructing a P-type tracking controller.

This article has been accepted for publication in a future issue of this journal, but has not been fully edited. Content may change prior to final publication. Citation information: DOI10.1109/TSMC.2023.3290011 IEEE Transactions on Systems, Man, and Cybernetics: Systems

The following P-type tracking controller is developed to guarantee that the controlled output of system (1) tracks the controlled output of system (9):

$$u(h) = \mathscr{K}\hbar(h) \tag{65}$$

where $\mathscr{K} \triangleq \begin{bmatrix} K_x & K_\chi \end{bmatrix}$ and K_x, K_χ are the controller gains to be determined.

In line with (11) and (65), we formulate the following augmented system:

$$\begin{aligned} \flat(h+1) =& \mathcal{A}_{[P]}\flat(h) + \mathcal{W}o(h) + \mathcal{T}_{[P]}\big(\bar{\xi}_0 + \tilde{\xi}_0(h)\big)\kappa_0(h) \\ &+ \mathcal{T}_{[P]}\big(\bar{\xi}_1 + \tilde{\xi}_1(h)\big)\kappa_1(h) + \mathcal{T}_{[P]}\big(\bar{\xi}_2 + \tilde{\xi}_2(h)\big)\kappa_2(h) \end{aligned} \tag{66}$$

where

$$\begin{aligned} \mathcal{A}_{[P]} \triangleq& \mathscr{A} + \mathscr{B}_{[P]}, \quad \mathcal{T}_{[P]} \triangleq \begin{bmatrix} BK_x \\ \mathbf{0} \end{bmatrix} \\ \mathscr{B}_{[P]} \triangleq& \begin{bmatrix} BK_xC & BK_\chi(C+H) \\ \mathbf{0} & \mathbf{0} \end{bmatrix}. \end{aligned}$$

In the sequel, we calculate the P-type controller parameters and present the minimal AUB of $\|z_\varepsilon(h)\|^2$ in the following corollary whose proof is easily accessible from those of Theorems 2-3.

Corollary 1: Let the positive scalar $\tilde{\omega}_1$ be given. Assume that there exist positive scalars $\tilde{\omega}_2$, $\tilde{\omega}_3$, $\tilde{\omega}_4$, $\tilde{\omega}_5$, positive definite matrices $\tilde{U}_{[1]}$, $\tilde{U}_{[2]}$ and matrices $\tilde{Y}_{[1]}$, $\tilde{Y}_{[2]}$, $\tilde{Y}_{[3]}$, $\tilde{K}_x$, $\tilde{K}_\chi$ such that the following inequality holds:

$$\Delta_4 = \begin{bmatrix} \Delta_4^{[1]} & \star \\ \Delta_4^{[2]} & \Delta_4^{[3]} \end{bmatrix} < 0 \tag{67}$$

where

$$\begin{aligned} \Delta_4^{[1]} \triangleq& \mathrm{diag}\{-\tilde{U} + \tilde{\omega}_1\tilde{U},\ -\tilde{\omega}_2\mathbf{I},\ -\tilde{\omega}_3\mathbf{I},\ -\tilde{\omega}_4\mathbf{I},\ -\tilde{\omega}_5\mathbf{I}\} \\ \Delta_4^{[2]} \triangleq& \begin{bmatrix} \tilde{\mathcal{A}}_{[P]} & \tilde{\mathcal{W}} & \bar{\xi}_0\tilde{\mathcal{T}}_{[P]} & \bar{\xi}_1\tilde{\mathcal{T}}_{[P]} & \bar{\xi}_2\tilde{\mathcal{T}}_{[P]} \end{bmatrix} \\ \Delta_4^{[3]} \triangleq& \mathrm{diag}\{\tilde{U}_{[1]} - \tilde{Y}_{[\Upsilon]} - \tilde{Y}_{[\Upsilon]}^T, -\tilde{U}_{[2]}\}, \tilde{U} \triangleq \mathrm{diag}\{\tilde{U}_{[1]},\ \tilde{U}_{[2]}\} \\ \tilde{Y} \triangleq& \begin{bmatrix} \tilde{Y}_{[1]} & \tilde{Y}_{[2]} \\ \mathbf{0} & \tilde{Y}_{[3]} \end{bmatrix}, \quad \tilde{\mathcal{W}} \triangleq \begin{bmatrix} \tilde{Y}_{[\Upsilon]}M & -\tilde{Y}_{[\Upsilon]}G \\ \mathbf{0} & \tilde{U}_{[2]}G \end{bmatrix} \\ \tilde{\mathcal{A}}_{[P]} \triangleq& \tilde{\mathscr{A}}_{[P]} + \tilde{\mathscr{B}}_{[P]},\ \tilde{\mathcal{T}}_{[P]} \triangleq \begin{bmatrix} K_x^{[\Upsilon]} \\ \mathbf{0} \end{bmatrix},\ \tilde{Y}_{[\Upsilon]} \triangleq \tilde{Y}\Upsilon \\ \tilde{\mathscr{A}}_{[P]} \triangleq& \begin{bmatrix} \tilde{Y}_{[\Upsilon]}A & \tilde{Y}_{[\Upsilon]}(A-F) \\ \mathbf{0} & \tilde{U}_{[2]}F \end{bmatrix}, \quad K_x^{[\Upsilon]} \triangleq \begin{bmatrix} \tilde{K}_x \\ \mathbf{0} \end{bmatrix} \\ \tilde{\mathscr{B}}_{[P]} \triangleq& \begin{bmatrix} K_x^{[\Upsilon]}C & K_\chi^{[\Upsilon]}(C+H) \\ \mathbf{0} & \mathbf{0} \end{bmatrix}, \quad K_\chi^{[\Upsilon]} \triangleq \begin{bmatrix} \tilde{K}_\chi \\ \mathbf{0} \end{bmatrix}. \end{aligned}$$

Then, the output tracking error dynamics $z_\varepsilon(h)$ is EUBMS. Additionally, the minimum of the AUB of $\|z_\varepsilon(h)\|^2$ can be obtained by solving the following minimization problem:

$$\begin{aligned} \min \quad & (\hbar^2\breve{\omega}_3 + 25\breve{\omega}_4 + \breve{\omega}_5)\sum_{s=1}^{p_y}\frac{\varpi_s^2 r_s^2}{l_s^2} + \omega_2(\bar{v}^2 + \bar{\mu}^2) \\ & \text{subject to} \ \ (67). \end{aligned} \tag{68}$$

Correspondingly, the desired controller gain matrices are given by

$$K_x = \tilde{Y}_{[1]}^{-1}\tilde{K}_x, \quad K_\chi = \tilde{Y}_{[1]}^{-1}\tilde{K}_\chi. \tag{69}$$

IV. Numerical Simulation

In this section, let us demonstrate the effectiveness and superiority of the developed PID tracking controller via a numerical simulation.

Consider a discrete linear time-invariant system of the form (1) with the following parameters:

$$\begin{aligned} A =& \begin{bmatrix} 1.01 & 0.1 \\ 0.2 & 0.4 \end{bmatrix}, \quad B = \begin{bmatrix} 0.156 \\ 0.42 \end{bmatrix}, \quad M = \begin{bmatrix} 0.45 \\ 0.82 \end{bmatrix} \\ C =& \begin{bmatrix} 1.01 & 0.5 \end{bmatrix}, \quad E = \begin{bmatrix} 1.1 & 0.3 \end{bmatrix}. \end{aligned}$$

Additionally, the parameters of the reference system in the form of (9) are given as follows:

$$F = \begin{bmatrix} 0.3 & 0.1 \\ 0.2 & 0.5 \end{bmatrix}, \quad G = \begin{bmatrix} 0.5 \\ 0.3 \end{bmatrix}, \quad H = \begin{bmatrix} 1 \\ 0.5 \end{bmatrix}^T.$$

Throughout all simulations, we set the initial values of (1) and (9) as $x(0) = \begin{bmatrix} 1.5 & -2.5 \end{bmatrix}^T$ and $\chi(0) = \begin{bmatrix} 0 & 0 \end{bmatrix}^T$; the exogenous disturbance as $v(h) = 0.1\sin(0.1h)$; and the reference input as

$$\mu(h) = \begin{cases} 0.1\sin(0.1h), & 0 \leqslant h \leqslant 150 \\ 0.05\sin(0.5h), & 200 \leqslant h \leqslant 400 \\ 0, & \text{otherwise.} \end{cases}$$

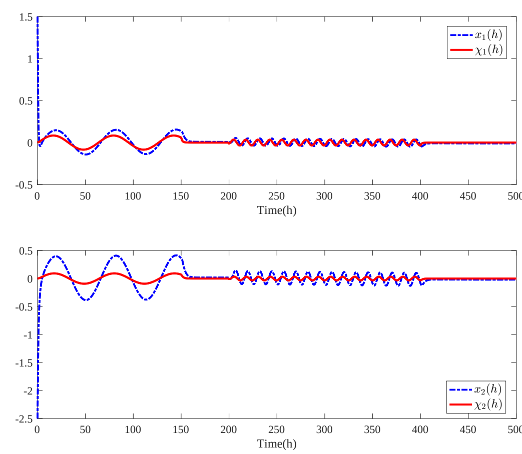

Fig. 3: Trajectories of $x(h)$ and $\chi(h)$.

In the simulation, the parameters of scalar quantizer (14) are chosen as $l_1 = 20$ and $r_1 = 17$. Making use of above parameters, the PID controller gains are computed via Theorem 3 and the obtained simulation results are demonstrated in Figs. 3–4. To be specific, Fig. 3 shows the state evolutions of the controlled system (1) and the reference system (9), and Fig. 4 depicts the controlled output of the controlled system (1) and the reference system (9). These illustrated simulation results obviously show that the controlled system achieves a desired tracking performance, which implies that the addressed PID tracking controller is indeed effective.

Additionally, in order to show the superiority of the developed PID tracking controller, we compare the tracking

This article has been accepted for publication in a future issue of this journal, but has not been fully edited. Content may change prior to final publication. Citation information: DOI10.1109/TSMC.2023.3290011 IEEE Transactions on Systems, Man, and Cybernetics: Systems

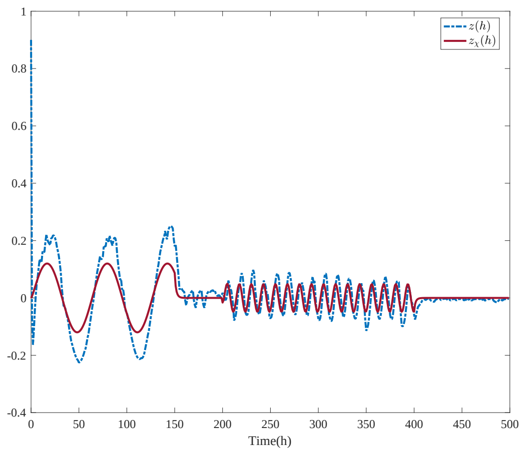

Fig. 4: Trajectories of $z(h)$ and $z_\chi(h)$.

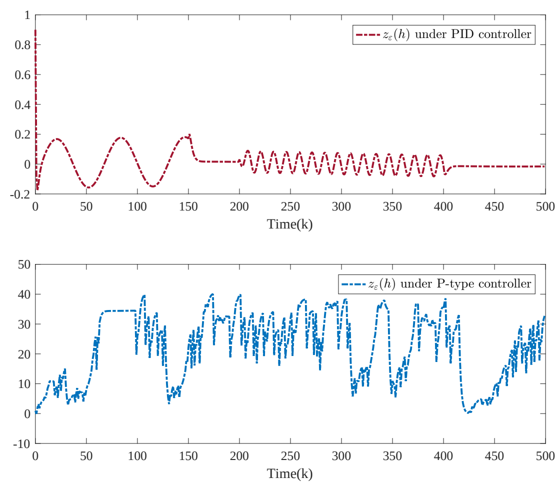

Fig. 5: Trajectory of $z_\varepsilon(h)$ under PID and P-type controller.

TABLE I: The minimum upper bounds of output tracking error and decoding error subject to different $\bar{\phi}_1$ for $\bar{\phi}_2 = 0.01$

$\bar{\phi}_1$	Minimum upper bounds of output tracking error	Minimum upper bounds of decoding error
0.99	0.117	0.111
0.89	0.144	0.119
0.79	0.191	0.121
0.69	0.269	0.124
0.59	0.282	0.135
0.49	0.543	0.142
0.39	0.555	0.161
0.29	0.594	0.174
0.19	0.407	0.185
0.09	0.412	0.197

performances between the PID tracking controller and the P-type tracking controller. Fig. 5 sketches the trajectories of the output tracking error under PID controller and P-type controller, respectively. One observers explicitly from these simulation results that the proposed PID controller performs better in providing satisfactory tracking performance compared to the P-type controller.

TABLE II: The minimum upper bounds of output tracking error and decoding error subject to different $\bar{\phi}_1$ for $\bar{\phi}_2 = 0.99$

$\bar{\phi}_1$	Minimum upper bounds of output tracking error	Minimum upper bounds of decoding error
0.91	0.027	0.041
0.81	0.039	0.056
0.71	0.048	0.068
0.61	0.054	0.071
0.51	0.059	0.076
0.41	0.072	0.088
0.31	0.077	0.094
0.21	0.086	0.098
0.11	0.098	1.102
0.01	0.111	0.105

At last, we discuss the influences from ROPDs on tracking performance and decoding accuracy. For different success rates $\bar{\phi}_1$ and $\bar{\phi}_2$ of description packet transmission, the minimum upper bounds of both output tracking error and decoding error are clearly outlined in Tables I-II after repeating the simulations 100 times, where the minimum upper bounds of both output tracking error and decoding error are increase with the decrease of $\bar{\phi}_1$ or $\bar{\phi}_2$. Accordingly, we can draw a conclusion that, as the description packet transmission success rates decrease, the tracking performance and decoding accuracy deteriorate.

V. Conclusions

In this paper, we have focused our attention on the PID tracking control problem in the presence of bounded disturbances. A MDEM has been implemented to enhance the reliability of the data transmission on the sensor-to-controller channels which are subject to ROPDs. A PID tracking controller has been constructed whose parameters have been elegantly designed by solving an optimization problem to minimize the upper bounds on tracking error. Further evaluation of the effect from the ROPDs on the decoding accuracy has been carried out by looking into the boundedness of the decoding error. Finally, a simulation example has been exploited to validate the effectiveness of the designed PID tracking controller. It is noted that one of the possible future research topics includes the extension of the developed MDED-based control scheme in this paper to more general complex networked systems (e.g. the multi-agent systems [4], the sensor networks [38] and the large-scale systems [20]).

References

[1] K. H. Ang, G. Chong and Y. Li, PID control system analysis, design, and technology, *IEEE Transactions on Control Systems Technology*, vol. 3, no. 4, pp. 559–576, Jul. 2005.

[2] K. J. Åström, T. Hägglund, C. C. Hang and W. K. Ho, Automatic tuning and adaptation for PID controllers-a survey, *Control Engineering Practice*, vol. 1, no. 4, pp. 699–714, Aug. 1993.

[3] H. Bai, M. Zhang, A. Wang, M. Liu and Y. Zhao, Multiple description video coding using inter- and intra-description correlation at macro block level, *IEICE Transactions on Information and Systems*, vol. E97-D, no. 2, pp. 384–387, Feb. 2014.

[4] G. Bao, L. Ma and X. Yi, Recent advances on cooperative control of heterogeneous multi-agent systems subject to constraints: A survey, *Systems Science & Control Engineering*, vol. 10, no. 1, pp. 539-551, Dec. 2022.

[5] Y. Berrouche and R. E. Bekka, Improved multiple description wavelet based image coding using Hadamard transform, *AEU-International Journal of Electronics and Communications*, vol. 68, no. 10, pp. 976–982, Oct. 2014.

[6] R. Caballero-Águila, A. Hermoso-Carazo and J. Linares-Pérez, Networked fusion estimation with multiple uncertainties and time-correlated channel noise, *Information Fusion*, vol. 54, pp. 161–171, Feb. 2020.

[7] R. Caballero-Águila, A. Hermoso-Carazo and J. Linares-Pérez, Networked distributed fusion estimation under uncertain outputs with random transmission delays, packet losses and multi-packet processing, *Signal Processing*, vol. 156, pp. 71–83, Mar. 2019.

[8] W. D. Chang and J. J. Yan, Adaptive robust PID controller design based on a sliding mode for uncertain chaotic systems, *Chaos, Solitons & Fractals*, vol. 26, no. 1, pp. 167–175, Oct. 2005.

[9] D. Ciuonzo, A. Aubry and V. Carotenuto, Rician MIMO channel- and jamming-aware decision fusion, *IEEE Transactions on Signal Processing*, vol. 65, no. 15, pp. 3866–3880, Aug. 2017.

[10] D. Ciuonzo, V. Carotenuto and A. De Maio, On multiple covariance equality testing with application to SAR change detection, *IEEE Transactions on Signal Processing*, vol. 65, no. 19, pp. 5078–5091, Oct. 2017.

[11] S. Cong and Y. Liang, PID-like neural network nonlinear adaptive control for uncertain multivariable motion control systems, *IEEE Transactions on Industrial Electronics*, vol. 56, no. 10, pp. 3872–3879, Oct. 2009.

[12] P. Correia, P. A. Assuncao and V. Silva, Multiple description of coded video for path diversity streaming adaptation, *IEEE Transactions on Multimedia*, vol. 14, no. 3, pp. 923–935, Jun. 2012.

[13] H. Du, S. Li and C. Qian, Finite-time attitude tracking control of spacecraft with application to attitude synchronization, *IEEE Transactions on Automatic Control*, vol. 56, no. 11, pp. 2711–2717, Nov. 2011.

[14] Z. Jin, V. Gupta and R. M. Murry, State estimation over packet dropping networks using multiple description coding, *Automatica*, vol. 42, no. 9, pp. 1441–1452, Sept. 2006.

[15] D. Kapetanovic, S. Chatzinotas and B. Ottersten, Index assignment for multiple description repair in distributed storage systems, in *Proceedings of the 2014 IEEE International Conference on Communications*, pp. 3896–3901, Sydney, Australia, Jun. 10–14, 2014.

[16] W. Li, Y. Niu and Z. Cao, Event-triggered sliding mode control for multi-agent systems subject to channel fading, *International Journal of Systems Science*, vol. 53, no. 6, pp. 1233–1244, 2022.

[17] Y. Li, S. Tong and T. Li, Observer-based adaptive fuzzy tracking control of MIMO stochastic nonlinear systems with unknown control directions and unknown dead zones, *IEEE Transactions on Fuzzy Systems*, vol. 23, no. 4, pp. 1228–1241, Aug. 2015.

[18] B. Niu, X. Zhao, L. Zhang and H. Li, p-times differentiable unbounded functions for robust control of uncertain switched nonlinear systems with tracking constraints, *International Journal of Robust and Nonlinear Control*, vol. 25, no. 16, pp. 2965–2983, Nov. 2015.

[19] Z.-H. Pang, L.-Z. Fan, Z. Dong, Q.-L. Han and G.-P. Liu, False data injection attacks against partial sensor measurements of networked control systems, *IEEE Transactions on Circuits and Systems II: Express Briefs*, vol. 69, no. 1, pp. 149–153, Jan. 2022.

[20] E. R. Pinto, E. G. Nepomuceno and A. S. L. O. Campanharo, Individual-based modelling of animal brucellosis spread with the use of complex networks, *International Journal of Network Dynamics and Intelligence*, vol. 1, no. 1, pp. 120–129, Dec. 2022.

[21] B. Qu, B. Shen, Y. Shen and Q. Li, Dynamic state estimation for islanded microgrids with multiple fading measurements, *Neurocomputing*, vol. 406, pp. 196–203, Sept. 2020.

[22] F. Qu, X. Zhao, X. Wang and E. Tian, Probabilistic-constrained distributed fusion filtering for a class of time-varying systems over sensor networks: a torus-event-triggering mechanism, *International Journal of Systems Science*, vol. 53, no. 6, pp. 1288–1297, 2022.

[23] M. A. Rana, F. Ndiaye, S. A. Chowdhury and N. Mansoor, Multiple description image transmission for diversity systems over unreliable communication networks, in *Proceedings of 10th International Conference on Computer and Information Technology*, pp. 240–244, Dhanmondi, Bangladesh, Dec. 27–29, 2007.

[24] S. Roshany-Yamchi, M. Cychowski, R. R. Negenborn, B. D. Schutter, K. Delaney and J. Connell, Kalman filter-based distributed predictive control of large-scale multi-rate systems: Application to power networks, *IEEE Transactions on Control Systems Technology*, vol. 21, no. 1, pp. 27–39, Jan. 2013.

[25] D. Rosinová and V. Veselý, Robust PID decentralized controller design using LMI, *International Journal of Computers Communications & Control*, vol. 2, no. 2, pp. 195–204, 2007.

[26] C. Shi, Z. Liu, X. Dong and Y. Chen, A novel error-compensation control for a class of high-order nonlinear systems with input delay, *IEEE Transactions on Neural Networks and Learning Systems*, vol. 29, no. 9, pp. 4077–4087, Sept. 2017.

[27] Y. S. Shmaliy, F. Lehmann, S. Zhao and C. K. Ahn, Comparing robustness of the Kalman, H_∞, and UFIR filters, *IEEE Transactions on Signal Processing*, vol. 66, no. 13, pp. 3447–3458, Jul. 2018.

[28] G. J. Silva, A. Datta and S. P. Bhattacharyya, New results on the synthesis of PID controllers, *IEEE Transactions on Automatic Control*, vol. 47, no. 2, pp. 241–252, Feb. 2002.

[29] J. Song, Y. Niu, J. Lam and H.-K. Lam, Fuzzy remote tracking control for randomly varying local nonlinear models under fading and missing measurements, *IEEE Transactions on Fuzzy Systems*, vol. 26, no. 3, pp. 1125–1137, Jun. 2018.

[30] G. Sun, L. Wu, Z. Kuang, Z. Ma and J. Liu, Practical tracking control of linear motor via fractional-order sliding mode, *Automatica*, vol. 94, pp. 221–235, Aug. 2018.

[31] R. H. C. Takahashi, P. L. D. Peres and P. A. V. Ferreira, Multiobjective H_2/H_∞ guaranteed cost PID design, *IEEE Control Systems Magazine*, vol. 17, no. 5, pp. 37–47, Oct. 1997.

[32] H. Tao, H. Tan, Q. Chen, H. Liu and J. Hu, H_∞ state estimation for memristive neural networks with randomly occurring DoS attacks, *Systems Science & Control Engineering*, vol. 10, no. 1, pp. 154–165, Dec. 2022.

[33] V. A. Vaishampayan, Design of multiple description scalar quantizers, *IEEE Transactions on Information Theory*, vol. 39, no. 3, pp. 821–834, May 1993.

[34] L. Wang, Z. Wang, B. Shen and G. Wei, Recursive filtering with measurement fading: A multiple description coding scheme, *IEEE Transactions on Automatic Control*, vol. 66, no. 11, pp. 5144–5159, Nov. 2021.

[35] L. Wang, S. Liu, Y. Zhang, D. Ding and X. Yi, Non-fragile $l_2 - l_\infty$ state estimation for time-delayed artificial neural networks: An adaptive event-triggered approach, *International Journal of Systems Science*, vol. 53, no. 10, pp. 2247–2259, Jul. 2022.

[36] X. Wang, Y. Sun and D. Ding, Adaptive dynamic programming for networked control systems under communication constraints: a survey of trends and techniques, *International Journal of Network Dynamics and Intelligence*, vol. 1, no. 1, pp. 85-98, Dec. 2022.

[37] G. Wei, W. Li, D. Ding and Y. Liu, Stability analysis of covariance intersection-based Kalman consensus filtering for time-varying systems, *IEEE Transactions on Systems, Man, and Cybernetics: Systems*, vol. 50, no. 11, pp. 4611–4622, Nov. 2020.

[38] P. Wen, X. Li, N. Hou and S. Mu, Distributed recursive fault estimation with binary encoding schemes over sensor networks, *Systems Science & Control Engineering*, vol. 10, no. 1, pp. 417–427, Dec. 2022.

[39] W. Xu, D. W. C. Ho, J. Zhong and B. Chen, Event/self-triggered control for leader-following consensus over unreliable network with DoS attacks, *IEEE Transactions on Neural Networks and Learning Systems*, vol. 30, no. 10, pp. 3137–3149, Oct. 2019.

[40] Y. Xu, Z. Yao, R. Lu and B. K. Ghosh, A novel fixed-time protocol for first-order consensus tracking with disturbance rejection, *IEEE Transactions on Automatic Control*, vol. 67, no. 11, pp. 6180–6186, Nov. 2022.

[41] Y. Xu, W. Lv, W. Lin, R. Lu and D. E. Quevedo, On extended state estimation for nonlinear uncertain systems with round-robin protocol, *Automatica*, vol. 138, Article 110154, 2022.

[42] T. Yang, F. Wu and L. Zhang, Tracking control of hybrid systems with state-triggered jumps and stochastic events and its application, *IET Control Theory & Applications*, vol. 11, no. 7, pp. 1024–1033, Apr. 2017.

[43] X.-M. Zhang, Q.-L. Han, X. Ge and L. Ding, Resilient control design based on a sampled-data model for a class of networked control systems

This article has been accepted for publication in a future issue of this journal, but has not been fully edited. Content may change prior to final publication. Citation information: DOI10.1109/TSMC.2023.3290011 IEEE Transactions on Systems, Man, and Cybernetics: Systems

under denial-of-service attacks, *IEEE Transactions on Cybernetics*, vol. 50, no. 8, pp. 3616–3626, Aug. 2020.

[44] X.-M. Zhang, Q.-L. Han and X. Yu, Survey on recent advances in networked control systems, *IEEE Transactions on Industrial Informatics*, vol. 12, no. 5, pp. 1740–1752, Oct. 2016.

[45] J. Zhang, X. He and D. Zhou, Filtering for stochastic uncertain systems with non-logarithmic sensor resolution, *Automatica*, vol. 89, pp. 194–200, Mar. 2018.

[46] Q. Zhang and Y. Zhou, Recent advances in non-Gaussian stochastic systems control theory and its applications, *International Journal of Network Dynamics and Intelligence*, vol. 1, no. 1, pp. 111–119, Dec. 2022.

[47] Z. Zhang, T. Leifeld and P. Zhang, Finite horizon tracking control of Boolean control networks, *IEEE Transactions on Automatic Control*, vol. 63, no. 6, pp. 1798–1805, Jun. 2017.

[48] Y. Zhang, N. Xia, Q.-L. Han and F. Yang, Set-membership global estimation of networked systems, *IEEE Transactions on Cybernetics*, vol. 52, no. 3, pp. 1454–1464, Mar. 2022.

Di Zhao received the B.Sc. degree in Mathematics from Jilin Normal University, Siping, China, in 2013 and the Ph.D. degree in Control Science and Engineering from University of Shanghai for Science and Technology, Shanghai, China, in 2020.

She is currently a Post-doctoral Research Fellow with the College of Science, University of Shanghai for Science and Technology, Shanghai, China. From November 2018 to November 2019, she was a visiting Ph.D. student in the Department of Computer Science, Brunel University London, Uxbridge, U.K. From March to June 2018, she was a Research Associate in the Department of Mathematics, City University of Hong Kong, Hong Kong. Dr. Zhao's research interests include PID control, proportional-integral observer, networked control systems and cyber-physical systems.

Dr. Zhao is currently a reviewer for some international journals.

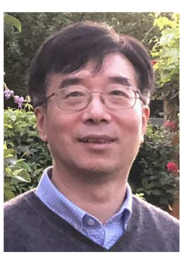

Zidong Wang (SM'03-F'14) was born in Jiangsu, China, in 1966. He received the B.Sc. degree in mathematics in 1986 from Suzhou University, Suzhou, China, and the M.Sc. degree in applied mathematics in 1990 and the Ph.D. degree in electrical engineering in 1994, both from Nanjing University of Science and Technology, Nanjing, China.

He is currently Professor of Dynamical Systems and Computing in the Department of Computer Science, Brunel University London, U.K. From 1990 to 2002, he held teaching and research appointments in universities in China, Germany and the UK. Prof. Wang's research interests include dynamical systems, signal processing, bioinformatics, control theory and applications. He has published more than 700 papers in international journals. He is a holder of the Alexander von Humboldt Research Fellowship of Germany, the JSPS Research Fellowship of Japan, William Mong Visiting Research Fellowship of Hong Kong.

Prof. Wang serves (or has served) as the Editor-in-Chief for *International Journal of Systems Science*, the Editor-in-Chief for *Neurocomputing*, the Editor-in-Chief for *Systems Science & Control Engineering*, and an Associate Editor for 12 international journals including IEEE Transactions on Automatic Control, IEEE Transactions on Control Systems Technology, IEEE Transactions on Neural Networks, IEEE Transactions on Signal Processing, and IEEE Transactions on Systems, Man, and Cybernetics-Part C. He is a Member of the Academia Europaea, a Member of the European Academy of Sciences and Arts, an Academician of the International Academy for Systems and Cybernetic Sciences, a Fellow of the IEEE, a Fellow of the Royal Statistical Society and a member of program committee for many international conferences.

Shuai Liu received the Ph.D. degree in system analysis and integration from the University of Shanghai for Science and Technology, Shanghai, China, in 2018.

From 2017 to 2018, she was a Visiting Ph.D. Student with the Department of Computer Science, Brunel University London, Uxbridge, U.K. She is currently an Associate Research Professor with the College of Science, University of Shanghai for Science and Technology, Shanghai, China. She was the recipient of the National Postdoctoral Innovative Talent Scholars of China. She has authored or coauthored more than 30 papers in refereed international journals. Her current research interests include sensor networks, complex networks, information fusion as well as Kalman filtering.

Dr. Liu is currently a reviewer for some international journals.

Qing-Long Han (M'09-SM'13-F'19) received the B.Sc. degree in mathematics from Shandong Normal University in 1983, and the M.Sc. and Ph.D. degrees in control engineering from East China University of Science and Technology, in 1992 and 1997, respectively. He is Pro Vice-Chancellor (Research Quality) and a Distinguished Professor at Swinburne University of Technology, Australia. He held various academic and management positions at Griffith University and Central Queensland University, Australia. His research interests include networked control systems, multi-agent systems, time-delay systems, smart grids, unmanned surface vehicles, and neural networks.

Professor Han was awarded The 2021 Norbert Wiener Award (the Highest Award in systems science and engineering, and cybernetics) and The 2021 M. A. Sargent Medal (the Highest Award of the Electrical College Board of Engineers Australia). He was the recipient of The 2022 IEEE Systems, Man, and Cybernetics Society Andrew P. Sage Best Transactions Paper Award, The 2021 IEEE/CAA Journal of Automatica Sinica Norbert Wiener Review Award, The 2020 IEEE Systems, Man, and Cybernetics Society Andrew P. Sage Best Transactions Paper Award, The 2020 IEEE Transactions on Industrial Informatics Outstanding Paper Award, and The 2019 IEEE Systems, Man, and Cybernetics Society Andrew P. Sage Best Transactions Paper Award.

Professor Han is a Member of the Academia Europaea (The Academy of Europe). He is a Fellow of The International Federation of Automatic Control (IFAC) and a Fellow of The Institution of Engineers Australia (IEAust). He is a Highly Cited Researcher in both Engineering and Computer Science (Clarivate Analytics). He has served as an AdCom Member of IEEE Industrial Electronics Society (IES), a Member of IEEE IES Fellows Committee, and Chair of IEEE IES Technical Committee on Networked Control Systems. Currently, he is Editor-in-Chief of *IEEE/CAA Journal of Automatica Sinica*, Co-Editor-in-Chief of *IEEE Transactions on Industrial Informatics*, and Co-Editor of *Australian Journal of Electrical and Electronic Engineering*.

Guoliang Wei received the B.Sc. degree in mathematics from Henan Normal University, Xinxiang, China, in 1997, and the M.Sc. degree in applied mathematics and the Ph.D. degree in control engineering from Donghua University, Shanghai, China, in 2005 and 2008, respectively.

He is currently a Professor with the Business School, University of Shanghai for Science and Technology, Shanghai, China. From March 2010 to May 2011, he was an Alexander von Humboldt Research Fellow with the Institute for Automatic Control and Complex Systems, University of Duisburg-Essen, Duisburg, Germany. From March 2009 to February 2010, he was a Postdoctoral Research Fellow with the Department of Information Systems and Computing, Brunel University, Uxbridge, U.K., sponsored by the Leverhulme Trust of the U.K. From June 2007 to August 2007, he was a Research Assistant with the University of Hong Kong, Hong Kong. From March 2008 to May 2008, he was a Research Assistant with the City University of Hong Kong, Hong Kong. He has published more than 100 papers in refereed international journals. His research interests include nonlinear systems, stochastic systems, and bioinformatics.

Prof. Wei is a very active reviewer for many international journals.